MATERNAL OBESITY CAUSES FETAL CARDIAC HYPERTROPHY AND ALTERS ADULT OFFSPRING MYOCARDIAL METABOLISM IN MICE

Owen R. Vaughan[1], Fredrick J. Rosario[1], Jeannie Chan[2], Laura A. Cox[2], Veronique Ferchaud-Roucher[1], Karin A. Zemski-Berry[3], Jane E.B. Reusch[3], Amy C. Keller[3], Theresa L. Powell[1,4] and Thomas Jansson[1]

[1]Department of Obstetrics and Gynecology, University of Colorado Anschutz Medical Campus, Aurora, CO, USA

[2]Department of Molecular Medicine, Wake Forest School of Medicine, Winston-Salem, NC, USA

[3]Department of Medicine, Division of Endocrinology, Metabolism and Diabetes, University of Colorado Anschutz Medical Campus, Aurora, CO, USA and Rocky Mountain Regional VA Medical Center, Aurora, CO, USA

[4]Department of Pediatrics, University of Colorado Anschutz Medical Campus, Aurora, CO, USA

Running title: Maternal obesity alters offspring heart metabolism

Manuscript category: Original article

Correspondence:

Owen R. Vaughan, PhD

Department of Obstetrics and Gynecology

University of Colorado Anschutz Medical Campus

12700 E19th Avenue

Aurora, CO, USA

owen.vaughan@CUAnschutz.edu

Phone: (303) 724-8622

Fax: (303) 724-3512

Table of Contents category: Placenta, Pregnancy and Perinatal Physiology.

Total word count: 5416 words

Key words: diabetes mellitus, gestational; fetal macrosomia; peroxisome proliferator activated receptor gamma; positron emission tomography; heart failure, diastolic

This manuscript was first published as a preprint: Vaughan, OR, Rosario FJ, Chan, J, Cox, LA, Ferchaud-Roucher, V, Zemski-Berry, KA, Reusch, JEB, Keller, AC, Powell, TL and Jansson, T (2021) *Maternal obesity causes fetal cardiac hypertrophy and alters adult offspring myocardial metabolism in mice.* bioRxiv 2021.09.15.460457; doi: https://doi.org/10.1101/2021.09.15.460457

KEY POINTS SUMMARY

- Obesity in pregnant women causes cardiac dysfunction in the fetus and increases lifelong cardiovascular disease risk in the offspring.
- In this study, we showed that maternal obesity in mice induces hypertrophy of the fetal heart in association with altered expression of genes related to nutrient metabolism.
- Maternal obesity also altered cardiac metabolism of carbohydrates and lipids in the adult offspring.
- The results suggest that overnutrition *in utero* may contribute to increased cardiovascular disease risk in children of women with obesity.

ABSTRACT

Obesity in pregnant women causes fetal cardiac dysfunction and increases offspring cardiovascular disease risk but its effect on myocardial metabolism is unknown. We hypothesised that maternal obesity alters fetal cardiac expression of metabolism-related genes and shifts offspring myocardial substrate preference from glucose towards lipids. Female mice were fed control or obesogenic diets before and during pregnancy. Fetal hearts were studied in late gestation (embryonic day, E18.5; term≈E21) and offspring were studied at 3, 6, 9 or 24 months postnatally. Maternal obesity increased heart weight and peroxisome proliferator activated receptor γ (*Pparg*) expression in female and male fetuses and caused left ventricular diastolic dysfunction in the adult offspring. Cardiac dysfunction progressively worsened with age in female, not male, offspring of obese dams, compared to age-matched controls. In 6-month-old offspring, exposure to maternal obesity increased cardiac palmitoyl carnitine-supported mitochondrial respiration in males and reduced myocardial ^{18}F-fluorodeoxyglucose uptake in females. Cardiac *Pparg* expression remained higher in adult offspring of obese than control dams and correlated with contractile and metabolic function. Maternal obesity did not affect cardiac palmitoyl carnitine respiration in females or ^{18}F-fluorodeoxyglucose uptake in males, or alter cardiac ^{3}H-oleic acid uptake, pyruvate respiration, lipid content or fatty acid/glucose transporter abundance in offspring of either sex. The results support our hypothesis and show that maternal obesity affects offspring cardiac metabolism in a sex-dependent manner. Persistent upregulation of *Pparg* expression in response to overnutrition *in utero* may mechanistically underpin programmed cardiac impairments and contribute to cardiovascular disease risk in children of women with obesity.

INTRODUCTION

The global prevalence of obesity in women of reproductive age is rapidly increasing (Poston *et al.*, 2016). Obesity in pregnant women predisposes their children to metabolic syndrome and a range of non-communicable diseases throughout life, thereby placing a substantial burden on the health of the population (Godfrey *et al.*, 2017). Children of women who have obesity during pregnancy are at 30% greater risk for cardiovascular disease in adulthood (Reynolds *et al.*, 2013). Diet-induced obesity in pregnant animals similarly leads to abnormal cardiovascular function in their adult offspring, irrespective of postnatal diet (Fernandez-Twinn *et al.*, 2012; Loche *et al.*, 2018), demonstrating that lifelong phenotype is programmed before birth. However, the mechanisms underlying cardiometabolic programming by maternal obesity remain poorly understood and neither the specific programming signals nor their primary targets in the fetus have been clearly identified.

Fetuses of obese women have cardiac hypertrophy and contractile dysfunction as early as the first trimester (Ece *et al.*, 2014; Ingul *et al.*, 2016), and these abnormalities persist at least into childhood (Toemen *et al.*, 2016). Similarly, in experimental animals, maternal obesity increases fetal heart size, wall thickness, cardiomyocyte size, inflammation and collagen content, and impairs contractility (Huang *et al.*, 2010; Wang *et al.*, 2010; Fan *et al.*, 2011; Kandadi *et al.*, 2013). These data suggest that maternal obesity directly affects the heart *in utero*.

Maternal obesity alters placental transport and fetal delivery of glucose and lipids, in both humans and experimental animals (Acosta *et al.*, 2015; Rosario *et al.*, 2015; Gázquez *et al.*, 2020; Powell *et al.*, 2021). Maternal obesity also increases fetal cardiac lipid storage in sheep (Kandadi *et al.*, 2013), and impairs glucose uptake and mitochondrial respiration in isolated cardiomyocytes from the offspring in rodents (Turdi *et al.*, 2013; Mdaki *et al.*, 2016). Impaired diastolic function in people with diabetes is associated with increased cardiac fatty acid uptake and oxidation, but reduced glucose uptake (Herrero *et al.*, 2006;

Rijzewijk *et al.*, 2009) whilst genetic modifications that increase cardiac lipid uptake and storage in mice cause contractile dysfunction (Son *et al.*, 2007). Whether abnormal cardiac glucose and lipid metabolism contributes to cardiac dysfunction in the offspring of pregnancies complicated by maternal obesity remains unknown.

We have developed a mouse model of maternal obesity associated with fetal overgrowth that closely replicates the phenotype of obese pregnant women in terms of maternal physiology, placental nutrient transport and fetal growth (Rosario *et al.*, 2015). In this model, administration of adiponectin to increase maternal concentrations of this metabolic hormone in obese dams, to the levels observed in control animals, normalises placental nutrient transport, prevents fetal overgrowth and mitigates cardiac diastolic dysfunction in the adult offspring (Aye *et al.*, 2015; Vaughan *et al.*, 2019). In the current study, we used the established model (Rosario *et al.*, 2015) to determine the effect of maternal obesity on the fetal cardiac transcriptome and on cardiac contractile and metabolic function in the adult offspring. We hypothesised that maternal obesity alters fetal cardiac expression of metabolism-regulating genes and increases lipid metabolism but reduces glucose metabolism in hearts of adult offspring. We measured cardiac metabolism in adult offspring of obese dams, relative to control offspring, at age 6 months, when diastolic dysfunction was apparent in both males and females (Vaughan *et al.*, 2019). We also quantified cardiac histone acetylation, which is linked to heart failure (Haberland *et al.*, 2009) and is sensitive to nutrient availability (Alrob *et al.*, 2014), to determine whether it plays a role in fetal cardiac programming by maternal obesity.

METHODS

Ethical approval

All procedures were conducted with approval from the Institutional Animal Care and Use Committee of the University of Colorado (protocol #00320)

Animals

Female C57BL6/J mice (Charles River Laboratories, MA, USA), proven breeders, were randomly assigned to receive an *ad libitum* obesogenic diet (Ob, n=31) consisting of high fat pellets (Western Diet D12079B, 41 kcal% fat) supplemented with sucrose solution (20 %), or a control diet (Con, D12489B, 10.6 kcal% fat, n=50). All animals had *ad libitum* access to fresh water and were housed under standard 12hr: 12hr dark:light conditions. When females fed the Ob diet had gained 25% of their initial body weight, they were mated overnight with stud males. Age-matched Con females were mated simultaneously. Successful mating was confirmed by the presence of a copulatory plug the following morning, designated embryonic day (E) 0.5 (term ~E19.5). Pregnant females were subsequently housed in pairs. On E18.5, a subset of Con (n=5) and Ob (n=5) dams were euthanised by CO_2 asphyxiation and cervical dislocation. The uterus was exposed, fetuses were excised and weighed then their hearts were dissected, weighed and snap frozen in liquid N_2. A fetal tail snip was also collected for subsequent determination of sex, by *Zfy-1* genotyping (Hacker *et al.*, 1995). For analyses of fetal tissues, all fetuses of each sex were pooled within each litter, so that the experimental unit was the dam. The remaining Con and Ob dams delivered naturally at term and continued to consume their respective diets throughout lactation, until all pups were weaned onto standard chow at age 4 weeks. Pups were subsequently housed in same sex groups, from multiple litters. In total, 187 offspring were used in the study. For postnatal analyses, each offspring was treated as an individual, so that the experimental unit was the pup. The median number of pups of each sex, from each litter used in postnatal studies was 2 (range 1 to 5).

Transcriptomic analyses

RNA extraction. Pooled heart tissues collected from male and female fetuses within litters from Con (n=5) and Ob (n=5) dams were stored at -80°C. Individual frozen tissue samples (~10 mg) were homogenized in TRI Reagent and total RNA was isolated using Direct-zol RNA MiniPrep kits (Zymo Research, Irvine, CA) according to the manufacturer's instructions. After eluting RNA from the Zymo-Spin column in 50 µl DNase/RNase-free water, RNA quality was assessed using an Agilent 2100 Bioanalyzer (Agilent Technologies, Inc., Santa Clara, CA). RNA concentration was quantified using Qubit RNA HS assay kits and a Qubit 2.0 Fluorometer (Thermo Fisher Scientific, Wilmington, DE). Total RNA was stored at -80°C.

RNA sequencing. Sequencing libraries with unique barcodes were constructed from 100 ng of total RNA using the KAPA Stranded mRNA-Seq kit (Kapa Biosystems, Wilmington, MA) according to the manufacturer's protocol. Individual cDNA libraries were quantified by qPCR. Pooled libraries were used to generate clusters by cBot with version 3 reagents (Illumina, San Diego, CA). Multiplex paired-end (2 x 100 base) sequencing was performed on the HiSeq 2500 Sequencing System with version 3 SBS chemistry (Illumina). Sequencing reads were demultiplexed using the CASAVA pipeline (Illumina) and then aligned to the *Mus musculus* reference genome (mm10) using STAR version 2.5.3a in Partek Flow (Partek, St. Louis, MO). Aligned reads were quantified using the Expectation/Maximization algorithm in Partek Flow with RefSeq transcripts from NCBI annotation release 84. Transcripts with zero read counts across all samples were removed prior to performing normalization of read counts using the Trimmed Mean of M-values method (Robinson & Oshlack, 2010). Afterwards, transcripts with at least 5 read counts across all samples were included for comparing expression in Ob vs. Con, separately in male and female fetuses. The Gene-Specific Analysis in Partek Flow was used for differential expression analysis, in which the best statistical model was identified for each transcript based on the normalized read counts of that transcript and the best model was used to produce the fold change, P values and P values adjusted by the method of Benjamini and Hochberg (Benjamini & Hochberg, 1995).

***Ingenuity Pathway Analysis*.** Differentially expressed mRNAs were functionally annotated *in silico* using Ingenuity Pathway Analysis (IPA) software (Qiagen). Downstream biological processes predicted to be affected by maternal obesity were identified using an unbiased approach based on significant enrichment with differentially expressed genes. The direction of expression change of mRNAs within each gene set was used to predict overall activation status of the pathway or function, by calculating a z-score, such that negative z-scores represented inhibited pathways and positive z-scores represented activated pathways. Functions were filtered for further investigation based on a threshold of z-score > |1.7| and ranked by significance level (P-value). Downstream functions commonly affected by maternal obesity in both female and male fetuses were identified using unsupervised comparative analysis in IPA. Unsupervised upstream regulator analysis within IPA was also used to identify key molecules (e.g. transcription factors) predicted to cause the observed transcriptional effects of multiple differentially expressed genes.

Experimental procedures

Echocardiography. Cardiac structure and function were assessed using transthoracic echocardiography in a subset of offspring at both 3 and 6 months of age (females n=10 Con, 6 Ob; males n= 7 Con, 7 Ob). Echocardiographic analyses for these animals only were reported previously (Vaughan *et al.*, 2019). Echocardiography was performed by an investigator blinded to the experimental group of each animal. Mice were anaesthetised (2% isoflurane, inhaled), placed in dorsal recumbency on a heated mat maintained at 37°C and hair removed from the thorax using a depilating cream. The heart was imaged in the parasternal short axis, at the level of the papillary muscle, by a trained operator blinded to the treatment group of the animal, using the Vevo 2100 system (VisualSonics). M-mode images of the left ventricle were collected across at least four consecutive cycles and used to measure ventricular wall thicknesses and chamber diameter in systole and diastole. Left ventricular internal volumes at systole and diastole were determined using the leading-edge method then ejection fraction and fractional shortening were calculated as indices of systolic function. Doppler velocimetry was used to determine peak mitral

inflow in early (E) and late (A) diastole whilst tissue Doppler was used to determine peak ventricular wall displacement at the level of the mitral annulus, again in early (E') and late (A') diastole. E/A, E'/A' and E/E' ratios were calculated as indices of ventricular diastolic function. Mice were recovered from anaesthesia following echocardiography and returned to their home cage.

One week after the second echocardiography assessment, offspring were fasted for 4 hr then euthanised by CO_2 asphyxiation and cervical dislocation. Hearts were perfused with PBS then excised and weighed. The left ventricle was dissected and snap frozen in liquid N_2 for gene expression analyses. Thirty-nine additional animals that had not undergone echocardiography were also euthanised at age 6 months, and tissues collected in the same manner for gene expression and lipidomic analyses.

Separate cohorts of offspring underwent echocardiographic assessment by the same operator at ages 9 months (n=28) or 24 months (n=22), without being imaged at earlier time points. These animals were euthanised seven days after echocardiography and their tissues collected for use in other studies.

Positron emission tomography. Cardiac glucose uptake was assessed *in vivo* in forty-eight 6-month old offspring using positron emission tomography (PET) with ^{18}F-fluorodeoxyglucose (^{18}F-FDG) tracer. Animals were fasted for 4 hours prior to the study then anaesthetised (2% isoflurane, inhaled) and positioned in dorsal recumbency on a warming pad at 37°C. Animals were then placed inside a PET imaging system (Inveon microPET, Siemens Medical, Knoxville, TN, USA) and a bolus dose of ^{18}F-FDG was administered intravenously, to the tail vein (250uCi). Fifteen dynamic PET image frames were collected at successive timepoints over a period of 35 minutes. A whole-body computerised tomography image, without contrast agent, was subsequently collected to confirm anatomical distribution of the ^{18}F-FDG tracer. Mice were removed from the scanner, recovered from anaesthesia and housed in a lead-shielded cage with *ad libitum* access to food and water, before being returned to their home cage 24 hr later.

Ten animals that underwent PET imaging were excluded from the subsequent analysis because (a) they did not tolerate anaesthesia, (b) poor tail vein patency hindered tracer infusion, or (c) movement interfered with collection of dynamic frame images. Dynamic frame PET images were assembled for each animal and voxel intensities (radioactivity) determined for manually defined regions of interest in the left ventricular myocardium (study compartment) and lumen (reference compartment). Radioactivity at each timepoint, within each compartment, was corrected for decay, animal weight and the amount of tracer injected. The ratio of radioactivity in the left ventricular myocardium to that in the reference compartment was then plotted against normalised time from tracer injection, according to the Patlak method (Zheng *et al.*, 2012). Separate linear regression lines were fitted to data from Con and Ob groups and the slopes compared by extra sum-of-squares F test, within each sex. The slope of the Patlak plot represents the clearance of ^{18}F-FDG from the blood, into the myocardium.

This group of animals was euthanised seven days after imaging, as described above. A portion of the left ventricle was placed into ice-cold biopsy preservation solution (BIOPS (Kuznetsov *et al.*, 2008)) for analysis of mitochondrial respiration within ~3 hours.

In vivo *left ventricular ^{3}H-oleic acid uptake.* Cardiac fatty acid uptake was quantified in 20 six-month old offspring using a radioactive tracer, as described previously (Son *et al.*, 2018). Briefly, 4.5µCi ^{3}H-oleic acid (NET289001MC, Perkin Elmer), was dried down under N_2 then resuspended in PBS and combined 1:1 with 40% fatty-acid free bovine serum albumin to a final volume of 200µl, at 37°C with shaking. Mice were anaesthetised with ketamine and xylazine (*i.p.*), the tail vein canulated and the BSA-complexed ^{3}H-oleic acid tracer delivered as a bolus. Up to five minutes later, mice were euthanised with sodium pentobarbital solution (*i.v.*), rapidly exsanguinated and the heart perfused with PBS. Plasma was separated from blood by centrifugation. Left ventricles (LV) were dissected, weighed then digested for 48 hr at 50°C in Biosol (National Diagnostics). LV and plasma radioactivity were determined by liquid scintillation counting and

220 ^{3}H-oleic acid clearance calculated from the ratio of total LV counts to the area under the curve of plasma
221 counts versus time from tracer infusion, divided by LV weight.

222 **Biochemical and molecular analyses**

223 ***High resolution in situ respirometry.*** Carbohydrate- and lipid supported rates of mitochondrial respiration
224 were assessed in cardiac muscle from 6-month old offspring, using high resolution respirometry. Biopsies
225 of fresh left ventricular tissue in ice-cold BIOPS solution were dissected under magnification into myofiber
226 bundles of approximately 1 mg. The sarcolemmal membrane was permeabilized by incubating in saponin
227 solution (40µg ml^{-1}, 20 min) then washed, accurately weighed and placed in an oxygraph chamber
228 (Oroboros O2k Respirometer), in respiration medium (MIRO5, (Kuznetsov *et al.*, 2008)) with blebbistatin
229 (5mM) to inhibit muscle contraction. Medium was equilibrated with O_2 gas to an initial dissolved
230 concentration of 400µM and the chamber was sealed. Catalase was also added to the respiration medium
231 to allow liberation of oxygen by H_2O_2 addition during the experiment, thus retaining dissolved O_2
232 concentration between 300 µM and 400 µM.

233 O_z consumption rate was determined during the sequential addition of one of two different combinations
234 of substrates and inhibitors, designed to determine the basal and maximal rates of carbohydrate- and
235 lipid-supported respiration, respectively. In the first assay, pyruvate (5mM) and malate (2mM) were
236 added to the oxygraph chamber to supply the electron transport chain via reduced intermediates
237 generated in the citric acid cycle. In the second assay, palmitoyl carnitine (5µM) and malate (1mM)
238 supplied electrons via mitochondrial β-oxidation. In both cases, leak state oxygen consumption was first
239 measured in the absence of ADP. Then ADP (2mM) was introduced to measure basal respiration rate,
240 coupled to ATP synthase activity. Glutamate (3mM) and succinate (6mM) were subsequently provided to
241 support direct electron flux to complex I and II of the electron transport chain, allowing maximum
242 oxidative phosphorylation capacity to be measured. ATP synthase activity was abolished using oligomycin

(4µg/ml), to measure leak state oxygen consumption supported by both fatty acid oxidation and direct complex I/II electron entry. Finally, FCCP (carbonyl cyanide 4-(trifluoromethoxy)phenylhydrazone) was added in increments of 0.5µM to permit free proton movement across the inner mitochondrial membrane, until maximal, uncoupled oxygen consumption was achieved, measuring electron transport chain capacity. Respiration rates were corrected to fresh tissue mass. Coupling efficiencies for each of the two combinations of substrates was calculated as 1 minus the ratio (leak state respiration/maximal electron transport chain capacity).

Targeted lipidomic analyses. Cardiac triglyceride contents were determined by colorimetric assay (MAK266, Sigma-Aldrich). Myocardial content of individual fatty acids, ceramides and diacylglycerol species was measured in adult offspring using targeted mass spectrometry. For total fatty acid quantification, frozen ventricular tissue was homogenised in hepes-tris buffered saline solution then lipids were extracted using a liquid-liquid extraction method, as described (Chassen et al, 2018). Briefly, an aliquot of ventricle homogenate was deproteinised by addition of methanol, with vortexing, then centrifuged (500g, 15 min, at room temperature). The supernatant solution was transferred to a glass vial, water and dichloromethane were added to extract lipids, vortexed and centrifuged. The polar lipid lower layer was separated and dichloromethane extraction was repeated with the upper aqueous layer. Combined lipid layers were dried under N_2, resuspended in ethanol then spiked with an internal FA standard solution. Lipids were saponified with 1M NaOH at 90°C for 1hr, neutralised, extracted into isooctane and derivatized using pentafluorobenzyl bromide and diisopropylethalamine in acetonitrile. The final fatty acid extract was resuspended in isooctane for GC-MS analysis. Samples were separated on a HP-5MS capillary column (30m, 0.25mm, 0.10mm film thickness, Agilent), subjected to mass spectrometry then identified and quantified based on *m/z* ratios and peak heights, respectively (Ferchaud-Roucher *et al.*, 2017).

For quantification of ceramides and diacylglycerol (DAG) species, heart samples homogenized in 900 µL water and an aliquot (20 µL) taken for protein concentration. Methanol (900 µL) was added to the homogenized sample (750 µL). After the addition of 15:0/18:1(d_7)-DAG (80 pmol) and 12:0-ceramide (80 pmol) as internal standards, lipid extraction was performed by the addition of methyl-*tert*-butyl ether (3 mL) according to Matyash et al (Matyash *et al.*, 2008). The organic phase was dried under a stream of nitrogen gas and resuspended in 400 µL of a mixture of 70/30 (v/v) hexane:methylene chloride. Samples were injected into an HPLC system connected to a triple quadrupole mass spectrometer (Sciex 2000 QTRAP, Framingham, MA) and normal phase chromatography with a HILIC column (100x2.1 mm, Kinetex HILIC 2.6 µm, Phenomenex) was used to separate lipids by class (Harrison & Bergman, 2019). Mass spectrometric analysis was performed in the positive ion mode using multiple-reaction monitoring (MRM) of DAG and ceramide molecular species and the internal standards. Quantitation was performed using stable isotope dilution with a standard curve for DAGs and ceramides and results were normalized to protein content. All lipid measurements were expressed relative to tissue protein content, determined by bicinchoninic acid assay.

Western blot. The abundances of fatty acid and glucose transporters, total and phosphorylated insulin receptor, and total and acetylated histones, were measured in cardiac tissue from 6-month old offspring using western blotting. Frozen heart samples were homogenised in hepes-tris buffered saline with protease and phosphatase inhibitors (Sigma Aldrich). Samples were then loaded in Laemmli buffer, resolved by polyacrylamide gel electrophoresis and transferred to polyvinylidene fluoride membrane. Membranes were incubated with primary antibodies to CD36, FATP1, FATP6, GLUT1, GLUT4 or total and acetylated (lysine-27 and lysine-9) histone H3, then with a horseradish peroxidase linked secondary antibody and visualised using enhanced chemiluminescence reaction and a gel imaging system. For analyses of insulin receptor abundance and phosphorylation, homogenised samples were resolved by

capillary electrophoresis (Jess, ProteinSimple, Bio-Techne, San Jose, CA, USA) and quantified using primary antibodies specific to total and phosphorylated (Tyr1361) insulin receptor β (Cell Signalling Technology, Danvers, MA, USA) and a fluorescently labelled secondary antibody. Protein abundance was determined by densitometry of specific bands, corrected for protein loading (amido black stain). The resultant arbitrary values for each sample were then normalised by dividing by the mean of the control group.

Gene expression. Cardiac expression of selected mRNAs related to lipid metabolism was determined in a targeted manner using qRT-PCR. RNA was extracted from frozen ventricular tissue from 6-month-old Con (females n=9, males n=11) and Ob (females n=10, males n=10) offspring using a commercially available kit (RNeasy Plus mini Kit, Qiagen) then reverse transcribed to cDNA (High Capacity cDNA Reverse Transcription kit, Applied Biosystems). Relative expression of target mRNAs was determined by qRT-PCR using SYBR Green chemistry and forward and reverse primers, as detailed in Table 1. The efficiency of all primer pairs was confirmed to be between 80 and 110% by calculating the linear gradient of the relationship between average Ct value and dilution factor for a 5-fold serially diluted standard curve of pooled cDNA. Gene expression was determined relative to the geometric mean of *Rna18s* and *Rps29* expression using the ddCt method.

Statistics.

Results are presented as mean ± SD. All statistical analyses were conducted separately in female and male offspring. Normality of data was assessed by Shapiro-Wilk test. Echocardiographic measurements of cardiac function and morphometry were analysed by two-way ANOVA, with maternal obesity and postnatal age as independent factors. When there was a significant interaction between these two factors, the simple effect of maternal obesity at each age was assessed by Sidak post-hoc test. The effect of offspring sex and its interaction with maternal obesity was also determined by two-way ANOVA, separately at each postnatal timepoint, for echocardiography data. For all other measurements, Con and

Ob groups were compared by Student's t-test or by Mann-Whitney test, if data did not conform to a normal distribution. Analyses of lipidomic data were corrected for multiple comparisons using the Holm-Sidak method. Linear relationships between variables were determined by Pearson's correlation. In all cases, significance was taken at the level $P<0.05$.

RESULTS

Maternal obesity in pregnant mice induces fetal cardiac hypertrophy and transcriptional activation of lipid metabolism genes

Maternal obesity increased fetal heart weight at E18.5, as a percentage of total body weight, in both male and female fetuses (Fig. 1A, B). Absolute heart and body weights were also greater in fetuses of obese dams, compared to controls (Table 2).

Maternal obesity concomitantly altered the expression of 841 genes in the hearts of female fetuses and 764 genes in the hearts of male fetuses, with 66 genes commonly altered in both sexes. Ingenuity analysis predicted inhibition of processes related to neoplasia and DNA repair/synthesis in male fetal hearts, and pathways related to function, quantity and movement of immune cells in female fetal hearts, in obese compared to control dams (z-score <-1.7, top ten functions by P-value, Fig. 1C, D). By contrast, maternal obesity activated synthesis of lipid and metabolism of membrane lipid derivatives in male fetuses, and uptake of monosaccharides and carbohydrates in female fetuses (activation z-score > 1.7, top-ten functions by P-value, Fig. 1 E, F). Transport of molecules was consistently activated by maternal obesity in both males and females (Fig. 1G).

The activated downstream functions related to molecular transport, carbohydrate and lipid metabolism encompassed an overlapping suite of differentially expressed genes, several of which were commonly regulated by maternal obesity in male and female fetuses (Fig. 1H). Specifically, maternal obesity upregulated *Pparg*, the nuclear peroxisome proliferator activated receptor implicated in lipogenesis (Montaigne *et al.*, 2021), *Cd36,* a plasma membrane fatty acid translocase, and *Prkaa1*, the catalytic subunit of cytoplasmic AMP-activated protein kinase (AMPKa1), in fetuses of both sexes (Fig. 1H-J). Network analysis of direct molecular interactions between the differentially expressed, metabolism-related genes indicated that *Pparg* was a critical node in both the female and male fetal transcriptomic

response (Fig. 1K, L). Furthermore, when unsupervised regulator effects analysis was used to link the annotated downstream functions of differentially expressed genes to upstream effectors, a network of genes activated by *Ppargc1a* and including *Cd36* and the triglyceride synthesis enzyme, *Lpin1*, was predicted to promote lipid synthesis in male fetal hearts in response to maternal obesity (Fig. 1M). Taken together, the transcriptomic data were most consistent with maternal obesity promoting cardiac lipid metabolism in male and female fetuses, by increasing expression of genes related to fatty acid uptake and lipid synthesis.

Maternal obesity in pregnant mice causes age- and sex-dependent diastolic dysfunction and left ventricular dilation in adult offspring.

In male offspring, E/A and E'/A' ratios of left ventricular diastolic function declined overall with increasing postnatal age from 3 to 24 months and were further impaired by maternal obesity at all time points (Fig. 2A, C). Maternal obesity also reduced E/E' ratio in males, with significant differences apparent between Con and Ob groups in both the youngest and oldest offspring studied (Fig. 2E). By contrast, the effect of maternal obesity on diastolic function in female offspring depended on the age at which they were studied. Three months after birth, neither E/A nor E'/A' ratio differed between Con and Ob female offspring (Fig 2B, D). Six months after birth, E'/A' ratio, but not E/A ratio, was reduced, and by 9 months both E'/A' and E/A ratios were lower in Ob compared to Con females. Finally, at age 24 months, E/A ratio was higher in Ob than Con female offspring, whereas E'/A' ratio was similar in the two groups, indicating a more severe state of diastolic dysfunction with pseudonormal filling pattern. E/E' ratio was lower in Ob than Con female offspring, irrespective of age (Fig. 2F). Therefore, maternal obesity caused diastolic dysfunction in adult offspring of both sexes, albeit the specific effect varied with age in males and females. The reduction in E'/A' ratio and E/A ratio with maternal obesity was significantly greater in female than male offspring at 9 months of age, but not at any other timepoint studied (Table 3).

In males, maternal obesity increased end-diastolic volume in 2-year-old offspring and increased end-systolic volume irrespective of age (Fig. 3A, C). By contrast, in female offspring, maternal obesity increased left ventricular end-diastolic volume, but not end-systolic volume (Fig. 3B, D). Both left ventricular wall thickness and systolic function, measured by ejection fraction and fractional shortening, increased modestly with age (main effect by two-way ANOVA $P<0.05$) in male and female mice but were not affected by maternal obesity ($P>0.05$, Table 4). When tissues were weighed at necropsy in 6-month old offspring, heart weight was significantly greater in Ob than Con females as an unadjusted value, but not expressed as a percentage of body weight (Table 5). However, none of the other measurements of body, heart or ventricle weight differed between Con and Ob offspring at this age.

Maternal obesity alters cardiac metabolism in adult offspring in a sex-specific manner

***Gene expression*.** Maternal obesity upregulated *Pparg* expression in both male and female 6-month old offspring of obese dams, compared to controls (Fig. 4A, B). *Cd36* and *Prkaa1* expression were also higher in Ob than Con male offspring hearts, but not in females (Fig. 4). In male offspring, maternal obesity increased expression of downstream *Pparg* targets related to lipid synthesis and storage (*Fasn, Plin2, Srebp1)* and lipid oxidation (*Ppargc1a, Cpt1b, Acox1*) but did not alter *Ppargc1b, Cpt1a, Acadm, Hoad, Pdk4* or *Ucp3* expression (Fig. 4A). In female offspring, maternal obesity upregulated *Fasn* but did not affect expression of any of the other downstream mediators of lipid metabolism studied (Fig. 4B). When adult male offspring from control and obese dams were combined, there was a strong inverse correlation between cardiac *Pparg* gene expression and E/E' ratio (Fig. 4C). In female offspring, there was a strong correlation between cardiac *Pparg* expression and left-ventricular end-diastolic volume (Fig. 4D). *Cd36* expression in female offspring also positively correlated with E/A ratio (Fig. 5) and inversely correlated with wall thickness at diastole, whilst both *Pdk4* and *Hoad* expression correlated with wall thickness at systole and *Hoad* correlated with end-diastolic volume (Fig. 5). There were no other significant correlations between cardiac gene expression and the measured echocardiographic and morphometric

387 outcomes in adult offspring (males n=13, females n=15). Therefore, transcriptional upregulation of *Pparg*
388 expression and lipid metabolism persisted in the offspring of obese dams and was linked to cardiac
389 functional and structural phenotype in male and female offspring.

390 ***Lipid metabolism*.** Left ventricular ^{3}H-oleic acid clearance *in vivo* was greater in female than male offspring
391 of control dams ($P<0.05$, t-test). However, cardiac fatty acid clearance did not differ significantly between
392 Ob offspring and their Con counterparts of the same sex (Fig. 6A, B). Maternal obesity reduced FATP6
393 transporter protein abundance in hearts of female, but not male offspring, and did not affect CD36 or
394 FATP1 protein abundance (Table 6, Fig. 7).

395 In male offspring, maternal obesity increased cardiac palmitoyl carnitine respiration in the leak state
396 (+oligomycin), when palmitoyl carnitine was supplied in combination with malate, glutamate and
397 succinate, supporting electron flux via mitochondrial complexes I and II (Fig. 6C). Maximal oxidative
398 phosphorylation-coupled palmitoyl carnitine respiration and electron transport chain capacity (+FCCP)
399 also tended ($P>0.05$) to be higher in Ob than Con male offspring hearts (Fig. 6C). However, maternal
400 obesity had no effect on either coupled or leak respiration supported by palmitoyl carnitine alone in male
401 offspring (Fig. 6C), or on any of the rates of fatty acid supported respiration in female offspring hearts (Fig.
402 6D). The coupling efficiency of fatty acid supported respiration correlated with cardiac *Pparg* expression
403 in male offspring (Fig. 6E). However, there were no overall differences in coupling efficiency between Con
404 and Ob offspring (Table 7).

405 Maternal obesity did not alter adult offspring cardiac total fatty acid content (females Con 17.3 ± 5.2
406 µmol/mg, Ob 14.1 ± 3.4 µmol/mg; males Con 15.5 ± 4.9 µmol/mg, Ob 14.9 ± 4.1 µmol/mg) or triglyceride
407 content (females Con 7.7 ± 7.3 µg/mg, Ob 9.3 ± 6.3 µg/mg; males Con 22.9 ± 16.7 µg/mg, Ob 32.7 ± 19.5
408 µg/mg). Maternal obesity reduced male offspring cardiac 1,2-18:2/18:1 DAG content (Con 52.3 ± 53.6
409 pmol/mg, Ob 17.5 ± 10.5 pmol/mg) but had no effect on any of the other DAGs measured in male or

female offspring hearts (P>0.05, data not shown). There was no difference in ceramide content between Con and Ob offspring (P>0.05, data not shown).

***Carbohydrate metabolism*.** Myocardial glucose uptake, determined using PET as the rate of clearance of ^{18}F-deoxyglucose from plasma into the left ventricle, was greater in male than female control offspring (P<0.05, t-test). Maternal obesity reduced myocardial glucose uptake in female but not male offspring (Fig. 8A-D) but did not alter cardiac GLUT1 or GLUT4 abundance in offspring of either sex (Table 6, Fig. 7). The abundance of phosphorylated (Tyr1361) insulin receptor β also tended to be lower in hearts of Ob versus Con female offspring (P=0.056, Table 6, Fig. 7). However, total insulin receptor β abundance was similar in the two groups of females and neither the total nor phosphorylated form was altered in male offspring (Table 6, Fig. 7). There were no differences between Con and Ob offspring in the rates of pyruvate-supported mitochondrial respiration in cardiac muscle *ex vivo* (Fig. 8E, F). Similarly, neither histone H3 protein abundance nor acetylation differed between Con and Ob offspring (Fig. 9).

DISCUSSION

This is the first study to determine the detailed effects of maternal obesity on fetal and offspring cardiac nutrient metabolism at both a molecular and functional level. The results show that maternal obesity causes fetal cardiac hypertrophy *in utero*, in association with transcriptomic changes consistent with altered cardiac carbohydrate and lipid metabolism. They also show that maternal obesity impairs cardiac diastolic function in both male and female adult offspring up to 2 years after birth. The impairments in contractile function were accompanied by persistent *Pparg* upregulation and altered carbohydrate and lipid metabolism in female and male offspring, respectively. The study therefore indicates that cardiac metabolism is programmed by *in utero* exposure to maternal obesity and contributes to cardiac dysfunction in later life.

The hypertrophic effects of maternal obesity on fetal heart and left ventricle weight were similar in female and male fetuses and consistent with that reported previously in other experimental animals (Huang *et al.*, 2010; Wang *et al.*, 2010; Fan *et al.*, 2011; Kandadi *et al.*, 2013) and pregnant women (Ece *et al.*, 2014; Ingul *et al.*, 2016). In contrast, the effect on the fetal cardiac transcriptome strongly depended on fetal sex, with less than 10% of the differentially expressed genes shared between females and males. Based on bioinformatic analysis of the differentially expressed genes, the gross hypertrophic effect did not appear to be explained by cellular processes that were transcriptionally inhibited in response to maternal obesity, which were broadly related to inflammation in female fetuses and cell proliferation in male fetuses. These changes could be linked to myocardial fibrotic remodelling (Huang *et al.*, 2010; Kandadi *et al.*, 2013) or impaired cardiomyocyte endowment, depending on fetal sex. However, the processes that were transcriptionally activated seemed more likely to contribute to cardiac hypertrophy, because they were associated with transport, uptake, synthesis and metabolism of macronutrient molecules required for cell growth and contractile function. Certainly, cardiac lipid and glucose metabolism are strongly linked to cardiac dysfunction in obese and diabetic adults (Herrero *et al.*, 2006; Rijzewijk *et al.*, 2009).

448 Our bioinformatic analysis pointed to *Pparg* as a central node in the network of differentially expressed
449 genes related to metabolism. Cardiac *Pparg* was upregulated in both female and male fetuses of obese
450 dams, consistent with previous reports in liver and skeletal muscle from fetuses of pregnant macaques
451 fed a high fat diet (Suter *et al.*, 2012; McCurdy *et al.*, 2016). The PPARγ protein is a transcription factor
452 that is activated by binding with fatty acid ligands and drives the expression of genes mediating fatty acid
453 uptake and oxidation, including fatty acid translocase *Cd36*, which was also upregulated in fetuses of
454 obese dams. *Pparg* mRNA expression is upregulated in adult mice fed a high fat diet (Vidal-Puig *et al.*,
455 1996) and cardiomyocyte-specific overexpression of *Pparg* causes cardiac hypertrophy in transgenic adult
456 mice, in association with systolic dysfunction, abnormal mitochondrial architecture, increased triglyceride
457 uptake and lipid storage and increased expression of genes encoding for proteins involved in β-oxidation
458 (Son *et al.*, 2007). Our previous study showed that maternal obesity increases placental lipid transport
459 and fetal lipid load in mice (Diaz *et al.*, 2015). Therefore, fetal cardiac hypertrophy in pregnancies
460 complicated by maternal obesity may be promoted by increased circulating fatty acid availability
461 activating PPARγ signalling in the heart.

462 The finding that maternal obesity impairs diastolic function in adult offspring up to 2 years old extends
463 our previous observations in this model (Vaughan *et al.*, 2019). These data confirm that transient cardiac
464 hypertrophy due to excess nutrition in early life leads to lasting impairments in contractile function of the
465 heart, in common with other studies in mice and their isolated cardiomyocytes (Turdi *et al.*, 2013; Loche
466 *et al.*, 2018). Since systolic function was not affected by maternal obesity, the echocardiographic
467 observations in offspring of obese dams were most consistent with the phenotype of heart failure with
468 preserved ejection fraction, which is a significant cause of cardiovascular mortality in people
469 (Vaduganathan *et al.*, 2017). Mild diastolic dysfunction is often subclinical and not diagnosed as heart
470 failure, but still associated with increased mortality (Redfield *et al.*, 2003). Our data therefore suggest
471 diastolic dysfunction or heart failure could be a contributing factor to increased later life cardiovascular

morbidity in people whose mothers had obesity during pregnancy (Reynolds *et al.*, 2013). To our knowledge, there have been no studies of adult cardiac function in this population.

In contrast with the changes in fetal heart weight, the effect of maternal obesity on offspring cardiac function depended on postnatal age and sex, with diastolic function consistently impaired in males but progressively worsening with age in females. This may be partly explained by circulating oestrogens having a cardioprotective effect in young female offspring (Wang *et al.*, 2015). The appearance of overt diastolic dysfunction in 9-month old offspring of obese dams, with both E'/A' and E/A ratios reduced, approximately coincided with declining oestradiol levels in this strain and may therefore reflect diminishment of the protective oestrogen effect (Nelson *et al.*, 1981). Unfortunately, we did not consider the influence of reproductive cycles in the timing of our analyses and blood collections, preventing us from further investigating the contribution of oestradiol levels. Female offspring of obese dams had most severe diastolic dysfunction at 2 years of age, which is certainly after full reproductive senescence occurs between 13 and 16 months (Nelson *et al.*, 1982). Sex differences in the long-term effect of maternal obesity on the offspring heart could therefore be due to sexually dimorphic changes in normal physiology and endocrinology with age. This is consistent with clinical observations showing that elderly women have a higher risk of cardiac dysfunction than men and are more likely to develop dysfunction in association with type 2 diabetes and ventricular hypertrophy (Ho *et al.*, 1993).

Our study suggests that the sex-specific effects of maternal obesity may also be linked to differences in the metabolism of the heart. The results provide the first demonstration that *in vivo* cardiac metabolism depends on sex in adult mice, with greater cardiac fatty acid uptake in females but greater glucose uptake in males, in line with the known differences between women and men (Peterson *et al.*, 2007; Kadkhodayan *et al.*, 2017). Reduced *in vivo* cardiac glucose uptake in adult female offspring of obese dams is consistent with the reported reduction in *in vitro* cardiomyocyte glucose uptake when the offspring of obese mice are fed a high fat diet (Turdi *et al.*, 2013). It also reflects the pathophysiological changes in the

hearts of people with type 2 diabetes (Rijzewijk *et al.*, 2009). Since there was no accompanying change in cardiac mitochondrial capacity for carbohydrate respiration or myocardial glucose transporter abundance, reduced cardiac glucose uptake may be explained by myocardial insulin resistance in female offspring of obese dams. Indeed, the trend for lower phosphorylation of insulin receptor β in the hearts of female offspring of obese dams may suggest cardiac insulin resistance occurring at the post-receptor level. Maternal obesity has been shown to cause peripheral insulin resistance, reduced cardiac insulin receptor abundance and sex-specific alterations in signalling pathways downstream of the insulin receptor in the offspring heart in other studies (Fernandez-Twinn *et al.*, 2012; Vaughan *et al.*, 2019). In turn, impaired glucose uptake may have limited cardiac flexibility to generate ATP under conditions of high workload or low oxygen, causing contractile dysfunction. Certainly, glucose uptake is positively correlated with systolic function in humans (Iozzo *et al.*, 2002).

Alterations in net cardiac lipid uptake did not explain diastolic dysfunction in the offspring of obese dams, even though myocardial fatty acid uptake has been reported to increase in association with diastolic dysfunction in people with diabetes (Rijzewijk *et al.*, 2009). Cardiac dysfunction in adult male offspring in our study may instead have been related to the increase in mitochondrial fatty acid oxidation, which similarly occurs in association with reduced energetic efficiency in the hearts of adult rats fed a high fat diet (Cole *et al.*, 2011). This effect may partly be mediated by increased expression of PPARγ co-activator 1α (*Pgc1a*), which stimulates mitochondrial biogenesis, and the carnitine acetyltransferase *Cpt1b*, responsible for trafficking long chain fatty acids into the mitochondria. Although our observations indicated that maternal obesity most robustly increased oligomycin-uncoupled β-oxidation, there was no accompanying increase in *Ucp3* expression or coupling control ratio, suggesting that the effect of maternal obesity was primarily due to increased activity of the β-oxidation pathway itself. Increased lipid oxidation in offspring of obese dams may have caused cardiomyocyte damage by increasing production of reactive oxygen species (Mdaki *et al.*, 2016). Despite increased *Plin2* and *Srebp1* expression in males, we did not

find evidence of increased cardiac lipid storage or altered abundance of DAG and ceramide derivatives, arguing against a role for cardiac lipotoxicity *per se* in the offspring of obese dams. This finding contrasted with previous studies in sheep fetuses and neonatal rats showing that maternal obesity increases cardiac lipid accumulation in the perinatal period (Fan *et al.*, 2011; Mdaki *et al.*, 2016). Increased lipid oxidation may therefore outweigh increased storage in the long term. Indeed, cardiac triglyceride content is reduced in adult offspring of pigs fed a high fat diet (Guzzardi *et al.*, 2018). The results are therefore most consistent with increased lipid oxidation underpinning cardiac dysfunction in male offspring of obese dams.

At a molecular level, increased cardiac lipid oxidation was consistent with the persistant upregulation of *Pparg* expression, compared to controls. We therefore speculate that *Pparg* upregulation causes the myocardial metabolic alterations and, in turn, diastolic dysfunction in the adult male offspring. This proposal is supported by the strong correlation of *Pparg* expression with E/E' ratio and respiratory coupling control ratio in adult male offspring. *Pparg* expression is strongly linked to increased locus specific H3K9 and H3K27 acetylation during adipogenesis (Mikkelsen *et al.*, 2010) and maternal high fat feeding increases fetal hepatic *Pparg* expression in association with increased histone acetylation (Aagaard-Tillery *et al.*, 2008) but we did not find any changes in total cardiac H3K9 and H3K27 acetylation in this study. Therefore, the epigenetic mechanism underpinning persisting upregulation of *Pparg* in the offspring of obese dams remains unclear.

Taken together, the results support our hypothesis that maternal obesity alters cardiac metabolism in fetuses and adult offspring of obese pregnant mice. They show that the long-term effects are sex-specific but associated with cardiac *Pparg* upregulation and a shift from glucose to lipid metabolism in both male and female offspring of obese dams. Reduced cardiac metabolic flexibility, established *in utero*, may therefore contribute to later-life cardiometabolic disease risk in children of women with obesity. The

findings imply that therapeutic strategies that modify the supply of nutrients to fetuses of obese women may improve their later health.

DATA AVAILABILITY STATEMENT

Data are available on request from the corresponding author, Owen Vaughan owen.vaughan@cuanschutz.edu

COMPETING INTERESTS

The authors declare no competing interests.

AUTHOR CONTRIBUTIONS

Conception or design: ORV, FJR, LAC, JEBR, TLP, TJ; acquisition, analysis or interpretation of data: ORV, FJR, JC, VF-R, KAZ-B, ACK; drafting the work or revising it critically for important intellectual content: ORV, TLP, TJ. All authors approved the final version of the manuscript, and agree to be accountable for all aspects of the work in ensuring that questions related to the accuracy or integrity of any part of the work are appropriately investigated and resolved. All persons designated as authors qualify for authorship, and all those who qualify for authorship are listed.

FUNDING

This work was supported by the Eunice Kennedy Shriver National Institute for Child Health and Human Development and National Center for Advancing Translational Sciences at the National Institutes of Health [grant numbers R24OD016724, R01HD065007, UL1 TR002535]. Lipidomics services were performed by the University of Colorado Nutrition Obesity Research Center Lipidomics Core Facility supported by National Institute of Diabetes and Digestive and Kidney Diseases [grant Number DK048520]. Contents are the authors' sole responsibility and do not necessarily represent official NIH views.

ACKNOWLEDGEMENTS

The authors would like to thank Kelsey Barner, Kate Erickson and Anita Kramer for technical assistance.

REFERENCES

Aagaard-Tillery KM, Grove K, Bishop J, Ke X, Fu Q, McKnight R & Lane RH. (2008). Developmental origins of disease and determinants of chromatin structure: maternal diet modifies the primate fetal epigenome. *Journal of Molecular Endocrinology* **41,** 91-102.

Acosta O, Ramirez VI, Lager S, Gaccioli F, Dudley DJ, Powell TL & Jansson T. (2015). Increased glucose and placental GLUT-1 in large infants of obese nondiabetic mothers. *Am J Obstet Gynecol* **212,** 227.e221-227.

Alrob OA, Sankaralingam S, Ma C, Wagg CS, Fillmore N, Jaswal JS, Sack MN, Lehner R, Gupta MP, Michelakis ED, Padwal RS, Johnstone DE, Sharma AM & Lopaschuk GD. (2014). Obesity-induced lysine acetylation increases cardiac fatty acid oxidation and impairs insulin signalling. *Cardiovasc Res* **103,** 485-497.

Aye IL, Rosario FJ, Powell TL & Jansson T. (2015). Adiponectin supplementation in pregnant mice prevents the adverse effects of maternal obesity on placental function and fetal growth. *Proc Natl Acad Sci U S A* **112,** 12858-12863.

Benjamini Y & Hochberg Y. (1995). Controlling the False Discovery Rate: A Practical and Powerful Approach to Multiple Testing. *Journal of the Royal Statistical Society: Series B (Methodological)* **57,** 289-300.

Cole MA, Murray AJ, Cochlin LE, Heather LC, McAleese S, Knight NS, Sutton E, Jamil AA, Parassol N & Clarke K. (2011). A high fat diet increases mitochondrial fatty acid oxidation and uncoupling to decrease efficiency in rat heart. *Basic research in cardiology* **106,** 447-457.

Diaz P, Harris J, Rosario FJ, Powell TL & Jansson T. (2015). Increased placental fatty acid transporter 6 and binding protein 3 expression and fetal liver lipid accumulation in a mouse model of obesity in pregnancy. *Am J Physiol Regul Integr Comp Physiol* **309,** R1569-1577.

Ece İ, Uner A, Balli S, Kibar AE, Oflaz MB & Kurdoglu M. (2014). The Effects of Pre-pregnancy Obesity on Fetal Cardiac Functions. *Pediatric Cardiology* **35,** 838-843.

Fan X, Turdi S, Ford SP, Hua Y, Nijland MJ, Zhu M, Nathanielsz PW & Ren J. (2011). Influence of gestational overfeeding on cardiac morphometry and hypertrophic protein markers in fetal sheep. *J Nutr Biochem* **22,** 30-37.

Ferchaud-Roucher V, Rudolph MC, Jansson T & Powell TL. (2017). Fatty acid and lipid profiles in primary human trophoblast over 90h in culture. *Prostaglandins, leukotrienes, and essential fatty acids* **121,** 14-20.

Fernandez-Twinn DS, Blackmore HL, Siggens L, Giussani DA, Cross CM, Foo R & Ozanne SE. (2012). The programming of cardiac hypertrophy in the offspring by maternal obesity is associated with hyperinsulinemia, AKT, ERK, and mTOR activation. *Endocrinology* **153,** 5961-5971.

Gázquez A, Prieto-Sánchez MT, Blanco-Carnero JE, Ruíz-Palacios M, Nieto A, van Harskamp D, Oosterink JE, Schierbeek H, van Goudoever JB, Demmelmair H, Koletzko B & Larqué E. (2020). Altered materno-fetal transfer of 13C-polyunsaturated fatty acids in obese pregnant women. *Clin Nutr* **39,** 1101-1107.

Godfrey KM, Reynolds RM, Prescott SL, Nyirenda M, Jaddoe VWV, Eriksson JG & Broekman BFP. (2017). Influence of maternal obesity on the long-term health of offspring. *The Lancet Diabetes & Endocrinology* **5,** 53-64.

Guzzardi MA, Liistro T, Gargani L, Ait Ali L, D'Angelo G, Rocchiccioli S, La Rosa F, Kemeny A, Sanguinetti E, Ucciferri N, De Simone M, Bartoli A, Festa P, Salvadori PA, Burchielli S, Sicari R & Iozzo P. (2018). Maternal Obesity and Cardiac Development in the Offspring: Study in Human Neonates and Minipigs. *JACC Cardiovasc Imaging* **11,** 1750-1755.

Haberland M, Montgomery RL & Olson EN. (2009). The many roles of histone deacetylases in development and physiology: implications for disease and therapy. *Nature Reviews Genetics* **10,** 32.

Hacker A, Capel B, Goodfellow P & Lovell-Badge R. (1995). Expression of Sry, the mouse sex determining gene. *Development* **121,** 1603-1614.

Harrison KA & Bergman BC. (2019). HPLC-MS/MS Methods for Diacylglycerol and Sphingolipid Molecular Species in Skeletal Muscle. *Methods Mol Biol* **1978,** 137-152.

Herrero P, Peterson LR, McGill JB, Matthew S, Lesniak D, Dence C & Gropler RJ. (2006). Increased myocardial fatty acid metabolism in patients with type 1 diabetes mellitus. *Journal of the American College of Cardiology* **47,** 598-604.

Ho KKL, Pinsky JL, Kannel WB & Levy D. (1993). The epidemiology of heart failure: The Framingham Study. *Journal of the American College of Cardiology* **22,** A6-A13.

Huang Y, Yan X, Zhao JX, Zhu MJ, McCormick RJ, Ford SP, Nathanielsz PW, Ren J & Du M. (2010). Maternal obesity induces fibrosis in fetal myocardium of sheep. *Am J Physiol Endocrinol Metab* **299,** E968-975.

Ingul CB, Loras L, Tegnander E, Eik-Nes SH & Brantberg A. (2016). Maternal obesity affects fetal myocardial function as early as in the first trimester. *Ultrasound in obstetrics & gynecology : the official journal of the International Society of Ultrasound in Obstetrics and Gynecology* **47,** 433-442.

Iozzo P, Chareonthaitawee P, Dutka D, Betteridge DJ, Ferrannini E & Camici PG. (2002). Independent association of type 2 diabetes and coronary artery disease with myocardial insulin resistance. *Diabetes* **51,** 3020-3024.

Kadkhodayan A, Lin CH, Coggan AR, Kisrieva-Ware Z, Schechtman KB, Novak E, Joseph SM, Davila-Roman VG, Gropler RJ, Dence C & Peterson LR. (2017). Sex affects myocardial blood flow and fatty acid substrate metabolism in humans with nonischemic heart failure. *Journal of nuclear cardiology : official publication of the American Society of Nuclear Cardiology* **24,** 1226-1235.

Kandadi MR, Hua Y, Zhu M, Turdi S, Nathanielsz PW, Ford SP, Nair S & Ren J. (2013). Influence of gestational overfeeding on myocardial proinflammatory mediators in fetal sheep heart. *J Nutr Biochem* **24,** 1982-1990.

Kuznetsov AV, Veksler V, Gellerich FN, Saks V, Margreiter R & Kunz WS. (2008). Analysis of mitochondrial function in situ in permeabilized muscle fibers, tissues and cells. *Nat Protoc* **3,** 965-976.

Loche E, Blackmore HL, Carpenter AAM, Beeson JH, Pinnock A, Ashmore TJ, Aiken CE, de Almeida-Faria J, Schoonejans J, Giussani DA, Fernandez-Twinn DS & Ozanne SE. (2018). Maternal Diet-Induced Obesity Programmes Cardiac Dysfunction in Male Mice Independently of Post-Weaning Diet. *Cardiovasc Res* **114,** 1372-1384.

Matyash V, Liebisch G, Kurzchalia TV, Shevchenko A & Schwudke D. (2008). Lipid extraction by methyl-tert-butyl ether for high-throughput lipidomics. *Journal of lipid research* **49,** 1137-1146.

McCurdy CE, Schenk S, Hetrick B, Houck J, Drew BG, Kaye S, Lashbrook M, Bergman BC, Takahashi DL, Dean TA, Nemkov T, Gertsman I, Hansen KC, Philp A, Hevener AL, Chicco AJ, Aagaard KM, Grove KL & Friedman JE. (2016). Maternal obesity reduces oxidative capacity in fetal skeletal muscle of Japanese macaques. *JCI insight* **1,** e86612.

Mdaki KS, Larsen TD, Wachal AL, Schimelpfenig MD, Weaver LJ, Dooyema SD, Louwagie EJ & Baack ML. (2016). Maternal high-fat diet impairs cardiac function in offspring of diabetic pregnancy through metabolic stress and mitochondrial dysfunction. **310,** H681-692.

Mikkelsen TS, Xu Z, Zhang X, Wang L, Gimble JM, Lander ES & Rosen ED. (2010). Comparative epigenomic analysis of murine and human adipogenesis. *Cell* **143,** 156-169.

Montaigne D, Butruille L & Staels B. (2021). PPAR control of metabolism and cardiovascular functions. *Nature Reviews Cardiology* **18,** 809-823.

Nelson JF, Felicio LS, Osterburg HH & Finch CE. (1981). Altered profiles of estradiol and progesterone associated with prolonged estrous cycles and persistent vaginal cornification in aging C57BL/6J mice. *Biol Reprod* **24,** 784-794.

Nelson JF, Felicio LS, Randall PK, Sims C & Finch CE. (1982). A longitudinal study of estrous cyclicity in aging C57BL/6J mice: I. Cycle frequency, length and vaginal cytology. *Biol Reprod* **27,** 327-339.

Peterson LR, Soto PF, Herrero P, Schechtman KB, Dence C & Gropler RJ. (2007). Sex Differences in Myocardial Oxygen and Glucose Metabolism. *Journal of nuclear cardiology : official publication of the American Society of Nuclear Cardiology* **14,** 573-581.

Poston L, Caleyachetty R, Cnattingius S, Corvalan C, Uauy R, Herring S & Gillman MW. (2016). Preconceptional and maternal obesity: epidemiology and health consequences. *The lancet Diabetes & endocrinology* **4,** 1025-1036.

Powell TL, Barner K, Madi L, Armstrong M, Manke J, Uhlson C, Jansson T & Ferchaud-Roucher V. (2021). Sex-specific responses in placental fatty acid oxidation, esterification and transfer capacity to maternal obesity. *Biochim Biophys Acta Mol Cell Biol Lipids* **1866,** 158861.

Redfield MM, Jacobsen SJ, Burnett JC, Jr., Mahoney DW, Bailey KR & Rodeheffer RJ. (2003). Burden of systolic and diastolic ventricular dysfunction in the community: appreciating the scope of the heart failure epidemic. *Jama* **289,** 194-202.

Reynolds RM, Allan KM, Raja EA, Bhattacharya S, McNeill G, Hannaford PC, Sarwar N, Lee AJ, Bhattacharya S & Norman JE. (2013). Maternal obesity during pregnancy and premature mortality from cardiovascular event in adult offspring: follow-up of 1 323 275 person years. *Bmj* **347,** f4539.

Rijzewijk LJ, van der Meer RW, Lamb HJ, de Jong HW, Lubberink M, Romijn JA, Bax JJ, de Roos A, Twisk JW, Heine RJ, Lammertsma AA, Smit JW & Diamant M. (2009). Altered myocardial substrate metabolism and decreased diastolic function in nonischemic human diabetic cardiomyopathy: studies with cardiac positron emission tomography and magnetic resonance imaging. *Journal of the American College of Cardiology* **54,** 1524-1532.

Robinson MD & Oshlack A. (2010). A scaling normalization method for differential expression analysis of RNA-seq data. *Genome Biology* **11,** R25.

Rosario FJ, Kanai Y, Powell TL & Jansson T. (2015). Increased placental nutrient transport in a novel mouse model of maternal obesity with fetal overgrowth. *Obesity* **23,** 1663-1670.

Son N-H, Park T-S, Yamashita H, Yokoyama M, Huggins LA, Okajima K, Homma S, Szabolcs MJ, Huang L-S & Goldberg IJ. (2007). Cardiomyocyte expression of PPARγ leads to cardiac dysfunction in mice. *The Journal of Clinical Investigation* **117,** 2791-2801.

Son NH, Basu D, Samovski D, Pietka TA, Peche VS, Willecke F, Fang X, Yu SQ, Scerbo D, Chang HR, Sun F, Bagdasarov S, Drosatos K, Yeh ST, Mullick AE, Shoghi KI, Gumaste N, Kim K, Huggins LA, Lhakhang T, Abumrad NA & Goldberg IJ. (2018). Endothelial cell CD36 optimizes tissue fatty acid uptake. *J Clin Invest* **128,** 4329-4342.

Suter MA, Chen A, Burdine MS, Choudhury M, Harris RA, Lane RH, Friedman JE, Grove KL, Tackett AJ & Aagaard KM. (2012). A maternal high-fat diet modulates fetal SIRT1 histone and protein deacetylase activity in nonhuman primates. *The FASEB Journal* **26,** 5106-5114.

Toemen L, Gishti O, van Osch-Gevers L, Steegers EA, Helbing WA, Felix JF, Reiss IK, Duijts L, Gaillard R & Jaddoe VW. (2016). Maternal obesity, gestational weight gain and childhood cardiac outcomes: role of childhood body mass index. *International journal of obesity (2005)* **40,** 1070-1078.

Turdi S, Ge W, Hu N, Bradley KM, Wang X & Ren J. (2013). Interaction between maternal and postnatal high fat diet leads to a greater risk of myocardial dysfunction in offspring via enhanced lipotoxicity, IRS-1 serine phosphorylation and mitochondrial defects. *Journal of Molecular and Cellular Cardiology* **55,** 117-129.

Vaduganathan M, Patel RB, Michel A, Shah SJ, Senni M, Gheorghiade M & Butler J. (2017). Mode of Death in Heart Failure With Preserved Ejection Fraction. *Journal of the American College of Cardiology* **69,** 556-569.

Vaughan OR, Rosario FJ, Powell TL & Jansson T. (2019). Normalisation of circulating adiponectin levels in obese pregnant mice prevents cardiac dysfunction in adult offspring. *International journal of obesity (2005)*.

Vidal-Puig A, Jimenez-Liñan M, Lowell BB, Hamann A, Hu E, Spiegelman B, Flier JS & Moller DE. (1996). Regulation of PPAR gamma gene expression by nutrition and obesity in rodents. *The Journal of clinical investigation* **97,** 2553-2561.

Wang J, Ma H, Tong C, Zhang H, Lawlis GB, Li Y, Zang M, Ren J, Nijland MJ, Ford SP, Nathanielsz PW & Li J. (2010). Overnutrition and maternal obesity in sheep pregnancy alter the JNK-IRS-1 signaling cascades and cardiac function in the fetal heart. *Faseb j* **24,** 2066-2076.

Wang YC, Xiao XL, Li N, Yang D, Xing Y, Huo R, Liu MY, Zhang YQ & Dong DL. (2015). Oestrogen inhibits BMP4-induced BMP4 expression in cardiomyocytes: a potential mechanism of oestrogen-mediated protection against cardiac hypertrophy. *British Journal of Pharmacology* **172,** 5586-5595.

Zheng X, Wen L, Yu S-J, Huang S-C & Feng DD. (2012). A study of non-invasive Patlak quantification for whole-body dynamic FDG-PET studies of mice. *Biomed Signal Process Control* **7,** 438-446.

775 **Table 1 Primer sequences used for qRT- PCR analysis of adult offspring hearts**

Target mRNA	Forward primer sequence	Reverse primer sequence
Pparg	GAGTGTGACGACAAGATTTG	GGTGGGCCAGAATGGCATCT
Cd36	AATGGCACAGACGCAGCCT	GGTTGTCTGGATTCTGGA
Prkaa1	GTCAAAGCCGACCCAATGATA	CGTACACGCAAATAATAGGGGTT
Pgc1a	TGTTCCCGATCACCATATTCC	TCCCGCTTCTCGTGCTCTTT
Pgc1b	AGGTGTTCGGTGAGATTGTA	TCAGATGTGGGATCATAGTCA
Cpt1a	CTCAGTGGGAGCGACTCTTCA	GGCCTCTGTGGTACACGACAA
Cpt1b	TTCAACACTACACGCATCCC	GCCCTCATAGAGCCAGACC
Mcad	GATGCATCACCCTCGTGTAAC	AAGCCCTTTTCCCCTGAAG
Hoad	GCAAAATCCAAGAAGGGAATTG	TGGTTGAAAGGCAGCTCAG
Pdk4	CCGCTGTCCATGAAGCA	GCAGAAAAGCAAAGGACGTT
Ucp3	CCAACATCACAAGAAATGC	TACAAACATCATCACGTTCC

776

777

Table 2 Effect of maternal obesity on body and heart weights in E18.5 fetuses

	Con	**Ob**	P value (t test)
Males	n=5 litters	n=5 litters	
Body weight (mg)	1050 ± 111	1272 ± 57	**0.004***
Heart weight (mg)	4.84 ± 1.25	7.64 ± 0.62	**0.002***
Females	n=5 litters	n=5 litters	
Body weight (mg)	995 ± 96	1228 ± 130	**0.012***
Heart weight (mg)	3.88 ± 0.59	7.14 ± 0.71	**<0.001***

Body and heart weights, determined at necropsy, in male and female fetuses of control (Con) and obese (Ob) dams. Litter mean values for Con and Ob groups compared by Student's t-test. *, $P<0.05$. Mean ± SD.

783 **Table 3. Interacting effects of offspring sex and maternal obesity on cardiac structure and function in 3- , 6-, 9- and 24-month old offspring.**

		P value		
	Age	Sex	Maternal obesity	Interaction
E'/A'	3 months	0.365	0.116	0.652
	6 months	***0.029***	***0.001***	0.161
	9 months	0.122	***<0.001***	***0.006***
	24 months	0.093	0.116	0.402
E/A	3 months	0.565	0.117	0.501
	6 months	0.775	***0.015***	0.945
	9 months	0.368	***<0.001***	***0.010***
	24 months	0.077	0.491	0.085
E/E'	3 months	0.571	***0.008***	0.775
	6 months	0.415	0.051	0.993
	9 months	0.067	0.188	0.160
	24 months	0.972	***<0.001***	0.395
LV vol diastole	3 months	***0.049***	***<0.001***	0.579
	6 months	***0.048***	***0.048***	0.076
	9 months	***0.004***	0.932	0.154
	24 months	0.870	0.137	0.161
LV vol systole	3 months	0.168	***0.030***	0.777
	6 months	0.057	0.088	0.677
	9 months	***<0.001***	0.607	0.643
	24 months	0.581	0.273	0.363
EF%	3 months	0.741	0.979	0.919
	6 months	0.906	0.331	0.389
	9 months	***<0.001***	0.286	0.375
	24 months	0.217	0.820	0.944
FS%	3 months	0.806	0.867	0.875
	6 months	0.730	0.341	0.367

	9 months	***<0.001***	0.320	0.333
	24 months	0.191	0.969	0.770
Wall thickness diastole	3 months	0.200	0.147	0.859
	6 months	***0.025***	0.384	0.660
	9 months	0.170	0.361	0.101
	24 months	0.430	0.753	0.651
Wall thickness systole	3 months	0.150	0.180	0.916
	6 months	***0.009***	0.261	0.125
	9 months	0.537	0.895	0.193
	24 months	0.128	0.400	0.699

784 Effects of sex and maternal obesity were determined separately at each postnatal age, by two-way ANOVA. P values given in table.

785

786 **Table 4 Effect of maternal obesity on left ventricular systolic function, morphology and heart rate in 3-, 6-, 9- and 24-month-old offspring.**

	Males					Females				
	Con	Ob	P value (two-way ANOVA)			Con	Ob	P value (two-way ANOVA)		
	n=5-7	n=5-13	Interaction	Age	Obesity	n=5-10	n=3-6	Interaction	Age	Obesity
Ejection fraction (%)										
3 months	62.2 ± 4.8	62.0 ± 4.7	0.782	0.041	0.242	62.6 ± 3.6	62.8 ± 5.1	0.994	0.001	0.826
6 months	61.6 ± 2.8	59.7 ± 2.8				60.6 ± 2.4	60.5 ± 3.5			
9 months	65.0 ± 2.4	61.9 ± 4.2				70.6 ± 0.7	70.3 ± 4.4			
24 months	66.0 ± 1.8	65.6 ± 8.5				63.2 ± 4.9	62.5 ± 4.2			
Fractional shortening (%)										
3 months	33.0 ± 3.3	33.0 ± 3.2	0.646	0.021	0.351	33.1 ± 2.6	33.4 ± 3.5	0.975	0.001	0.935
6 months	32.5 ± 2.0	31.2 ± 1.8				31.6 ± 1.6	31.6 ± 2.5			
9 months	35.1 ± 1.7	32.8 ± 3.1				39.2 ± 0.5	39.1 ± 3.6			
24 months	35.6 ± 1.3	36.1 ± 6.4				33.9 ± 3.4	33.3 ± 2.7			
Wall thickness at diastole (mm)										
3 months	0.52 ± 0.02	0.50 ± 0.03	0.091	0.001	0.523	0.51 ± 0.04	0.49 ± 0.02	0.55	0.001	0.655
6 months	0.55 ± 0.03	0.55 ± 0.03				0.51 ± 0.02	0.53 ± 0.05			
9 months	0.50 ± 0.04	0.56 ± 0.07				0.50 ± 0.03	0.48 ± 0.03			
24 months	0.62 ± 0.09	0.60 ± 0.03				0.59 ± 0.05	0.60 ± 0.03			
Wall thickness at systole (mm)										
3 months	0.73 ± 0.03	0.71 ± 0.03	0.241	0.001	0.715	0.71 ± 0.05	0.69 ± 0.02	0.424	0.001	0.379
6 months	0.78 ± 0.04	0.75 ± 0.02				0.72 ± 0.04	0.73 ± 0.03			
9 months	0.70 ± 0.04	0.74 ± 0.09				0.72 ± 0.04	0.68 ± 0.03			
24 months	0.88 ± 0.08	0.91 ± 0.08				0.85 ± 0.03	0.86 ± 0.04			
Heart rate (bpm)										
3 months	502 ± 37	504 ± 31	0.32	0.002	0.604	542 ± 40	521 ± 38	0.961	0.291	0.223
6 months	540 ± 28	521 ± 36				563 ± 40	544 ± 25			
9 months	525 ± 36	544 ± 31				557 ± 55	551 ± 50			
24 months	568 ± 27	547 ± 30				564 ± 30	553 ± 36			

787 Main effects of maternal obesity and postnatal age, and their interaction, were determined by two-way ANOVA . P values given in table. Mean ±
788 SD

Table 5 Effect of maternal obesity on body and heart weights in 6-month-old adult offspring

	Con	**Ob**	P value (t test)
Males	n=47	n=31	
Body weight (g)	36.4 ± 5.5	36.1 ± 5.8	0.830
Heart weight (mg)	158 ± 22	162 ± 25	0.527
(% body wt. x 1000)	4.40 ± 0.67	4.55 ± 0.88	0.405
LV weight (g)	112 ± 13	114 ± 19	0.623
(% body wt. x 1000)	3.08 ± 0.39	3.24 ± 0.70	0.289
Females	n=42	n=34	
Body weight (g)	26.8 ± 4.6	28.5 ± 5.1	0.149
Heart weight (mg)	127 ± 17	139 ± 25	0.012*
(% body wt. x 1000)	4.79 ± 0.63	4.97 ± 0.89	0.305
LV weight (g)	89.7 ± 12.3	93.9 ± 17.7	0.325
(% body wt. x 1000)	3.35 ± 0.33	3.44 ± 0.63	0.561

Body, heart and LV weight, determined at necropsy, in 6-month old male and female offspring of control (Con) and obese (Ob) dams. Con and Ob groups compared by Student's t-test. *, $P<0.05$. Mean ± SD.

Table 6 Effect of maternal obesity on cardiac abundance of fatty acid transporters, glucose transporters and insulin receptor in 6-month-old adult offspring

	Con	**Ob**	P value (t test)
Males	n=10	n=10	
CD36	1.00 ± 0.16	1.02 ± 0.19	0.748
FATP1	1.00 ± 0.73	0.90 ± 1.01	0.331[b]
FATP6	1.00 ± 0.75	1.25 ± 0.88	0.501
GLUT1	1.00 ± 0.32	1.18 ± 0.47	0.321
GLUT4	1.00 ± 0.37	1.12 ± 0.35	0.448
IR β	1.00 ± 0.23	1.12 ± 0.35	0.391
Phospho-IR β (Tyr1361)	1.00 ± 0.49	0.87 ± 0.86	0.223[b]
Females	n=10	n=10	
CD36	1.00 ± 0.15	0.95 ± 0.19	0.462
FATP1	1.00 ± 0.57	2.27 ± 2.12	0.143[a]
FATP6	1.00 ± 0.53	0.44 ± 0.19	**0.006[b]***
GLUT1	1.00 ± 1.01	0.88 ± 1.08	0.310[a]
GLUT4	1.00 ± 0.09	1.02 ± 0.16	0.746
IR β	1.00 ± 0.70	0.75 ± 0.38	0.370
Phospho-IR β (Tyr1361)	1.00 ± 0.42	0.66 ± 0.25	0.056

Relative transporter protein abundance in LV homogenates, determined by western blot, in 6-month old male and female offspring of control (Con) and obese (Ob) dams. Con and Ob groups compared by Student's t-test or Mann-Whitney test[a], as appropriate to distribution. [b]Log transformed prior to statistical analysis. *P<0.05. Mean ± SD. Values are fraction of control mean.

Table 7 Effect of maternal obesity on mitochondrial coupling efficiency in adult offspring

	Con	Ob	P value (t test)
Males	n=16	n=10	
Palmitoyl-carnitine supported respiration (%)	33.4 ± 8.1	31.5 ± 11.5	0.625
Pyruvate-supported respiration (%)	26.8 ± 7.5	23.2 ± 6.1	0.218
Females	n=15	n=9	
Palmitoyl-carnitine supported respiration (%)	29.0 ± 6.3	27.0 ± 7.0	0.475
Pyruvate-supported respiration (%)	28.4 ± 8.0	28.9 ± 8.1	0.871

Coupling efficiencies for each of the two combinations of substrates was calculated as 1 minus the ratio (leak state respiration/maximal electron transport chain capacity).

FIGURE LEGENDS

Fig. 1 Maternal obesity induces fetal cardiac hypertrophy in association with altered transcription of metabolic genes at E18.5.

(A, B) Heart weight, relative to body weight, in female and male fetuses of control (Con) and obese (Ob) dams, on E18.5 of gestation. Con and Ob groups compared by Student's t-test. P and n values given in figure. Bars are mean ± SD. Symbols represent mean values of all pups of each sex within one litter. (C – F) Top 10 biological processes, ranked by P value, predicted to be inhibited (C, D) or activated (E, F) in hearts of female and male fetuses of obese dams, based on Ingenuity Pathway Analysis of differential gene expression, compared to controls. Activation status determined by z-score >|1.7|. (G) Comparison of biological processes activated or inhibited in response to maternal obesity, in male and female fetuses. Color scale indicates activation z-score relative to control fetuses. (H) Comparison of metabolic genes differentially expressed in response to maternal obesity, in male and female fetuses. Color scale indicates differential expression relative to control fetuses. (I, J) Predicted effect of differentially expressed metabolic genes on downstream biological processes in hearts of female and male fetuses of obese dams. Color of molecules represents expression change Ob vs Con: magenta, upregulated; teal, downregulated. Color of arrows represents direction of predicted effect on downstream processes: orange, activation; grey, neutral; blue, inhibition; yellow, expression inconsistent with predicted activation. (K, L) Network analysis showing cellular location and direct molecular interactions of differentially expressed, metabolism-related genes in E18.5 male and female fetuses of obese dams. (M) Regulator effects network identified from differentially expressed genes in male fetuses of obese dams.

Fig. 2 Maternal obesity causes age- and sex-dependent left ventricular diastolic dysfunction in adult offspring.

Echocardiographic indices of diastolic function in 3- to 24-month old male (A, C, E) and female (B, D, F) offspring of control (white bars) and obese dams (grey bars). (A, B) Ratios of early- to late-diastolic left ventricular wall displacement determined by tissue Doppler (E'/A'). (C, D) Ratios of early- to late-diastolic mitral inflow determined by pulsed wave Doppler (E/A). (E, F) Ratio of early diastolic mitral inflow to wall displacement (E/E'). Main effects of maternal obesity and postnatal age, and their interaction, were determined by two-way ANOVA and P values given in figure. Post-hoc comparisons of Con and Ob groups at each age used the Sidak test; * P<0.05, ** P<0.01, ***P<0.001. Bars are mean ± SD. Symbols represent individual animals. n values given in bars.

Fig. 3 Maternal obesity causes age- and sex-dependent left ventricular dilatation in adult offspring.

Left ventricular end-diastolic and end-systolic volumes, determined by echocardiography, in 3- to 24-month old male (A, C) and female (B, D) offspring of control (white bars) and obese dams (grey bars). Main effects of maternal obesity and postnatal age, and their interaction, were determined by two-way ANOVA and P values given in figure. Post-hoc comparisons of Con and Ob groups at each age used the Sidak test; * P<0.05, ** P<0.01, ***P<0.001 Bars are mean ± SD. Points represent individual animals. n values given in figure.

Fig. 4 Maternal obesity increases cardiac expression of Pparg and its downstream targets in adult offspring.

Relative expression of candidate genes in left ventricles of 6-month old male (A, Con n=11, Ob n=10) and female (B, Con n=9, Ob n=10) offspring at age 6 months, determined by qPCR relative to *Rna18s* and *Rps29*. Bars are mean ± SD. Con and Ob offspring compared by Student's t-test.*, P<0.05. (C, D) Correlation of left ventricular *Pparg* expression with E/E' ratio in male offspring and end-diastolic volume in female offspring of Con and Ob dams. Relationship between variables assessed by Pearson's correlation, P, R and N values given in figure. Least-squares regression line shown.

Fig. 5 Correlations between cardiac expression of metabolism-related genes and echocardiographic indices in female offspring of control and obese dams.

Relative expression of candidate genes in left ventricles of 6-month old female (B, Con n=9, Ob n=10) offspring at age 6 months, determined by qPCR relative to *Rna18s* and *Rps29*. Relationship between variables assessed by Pearson's correlation, P, R and N values given in figure. Least-squares regression line shown.

Fig. 6 Maternal obesity increases myocardial fatty acid oxidation in adult male, but not female, offspring

(A, B) In vivo left ventricular 3H-oleic acid clearance in male (Con n=7, Ob n=4) and female (Con n=3, Ob n=6) offspring. (C, D) Palmitoyl carnitine-supported mitochondrial respiration rates in isolated, permeabilized cardiac myofibers from 6-month old male (Con n=16, Ob n=10) and female (Con n=16, Ob n=9) offspring of Con and Ob dams. Respiration rates and clearances compared between Con and Ob groups by Student's t-test, P values given in figure. Mean ± SD. Symbols represent individual offspring. (E) Correlation between palmitoyl carnitine supported coupling control ratio and Pparg expression in male

offspring. Relationship between variables determined by Pearson's correlation, P and R values in figure. Least-squares regression line shown.

Fig 7 Representative western blots for fatty acid transporter, glucose transporter and insulin receptor proteins in hearts of 6-month-old offspring of control and obese dams

C, offspring from control dam; O, offspring from obese dam. Amido black/total protein stains indicate protein loading.

Fig. 8 Maternal obesity impairs myocardial glucose uptake in adult female, but not male, offspring

(A-D) Left ventricular 8F-fluorodeoxyglucose clearance in male (Con n=8, Ob n=9) and female (Con n=10, Ob n=11) offspring of control and obese dams at age 6 months. Con and Ob groups compared by least-square linear regression of (A, C) Patlak plot, symbols represent mean ± SD values for all individuals within each group, at each normalized time point. (B, D) Histogram of mean ± SD clearance (gradient of Patlak plot) for each experimental group. (E, F) Pyruvate-supported mitochondrial respiration rates in isolated, permeabilized cardiac myofibers from 6-month old male (Con n=16, Ob n=10) and female (Con n=15, Ob n=9) offspring of control and obese dams. Con and Ob groups compared by Student's t test. P values for intergroup comparisons given in figure. Bars are mean + SD. Points represent individual animals.

Fig. 9 Maternal obesity does not affect myocardial histone H3 acetylation in adult offspring.

(A) Representative western blots for total and acetylated histones in male and female offspring of control (C) and obese (O) dams. Amido black stain indicates protein loading. (B-G) Relative protein abundance of total (B, C), acetyl-lysine-27 (D, E) and acetyl-lysine-9 (F, G) histone H3 in 6-month old male and female offspring of Con and Ob dams. Con and Ob groups compared by Student's t-test, P values given in figure. Bars are mean ± SD. Points represent individual animals. n values given in figure. Values are fraction of control mean.

Abstract figure. Schematic diagram illustrating experimental design and major findings.

Fig. 1 Maternal obesity induces fetal cardiac hypertrophy in association with altered transcription of metabolic genes at E18.5.

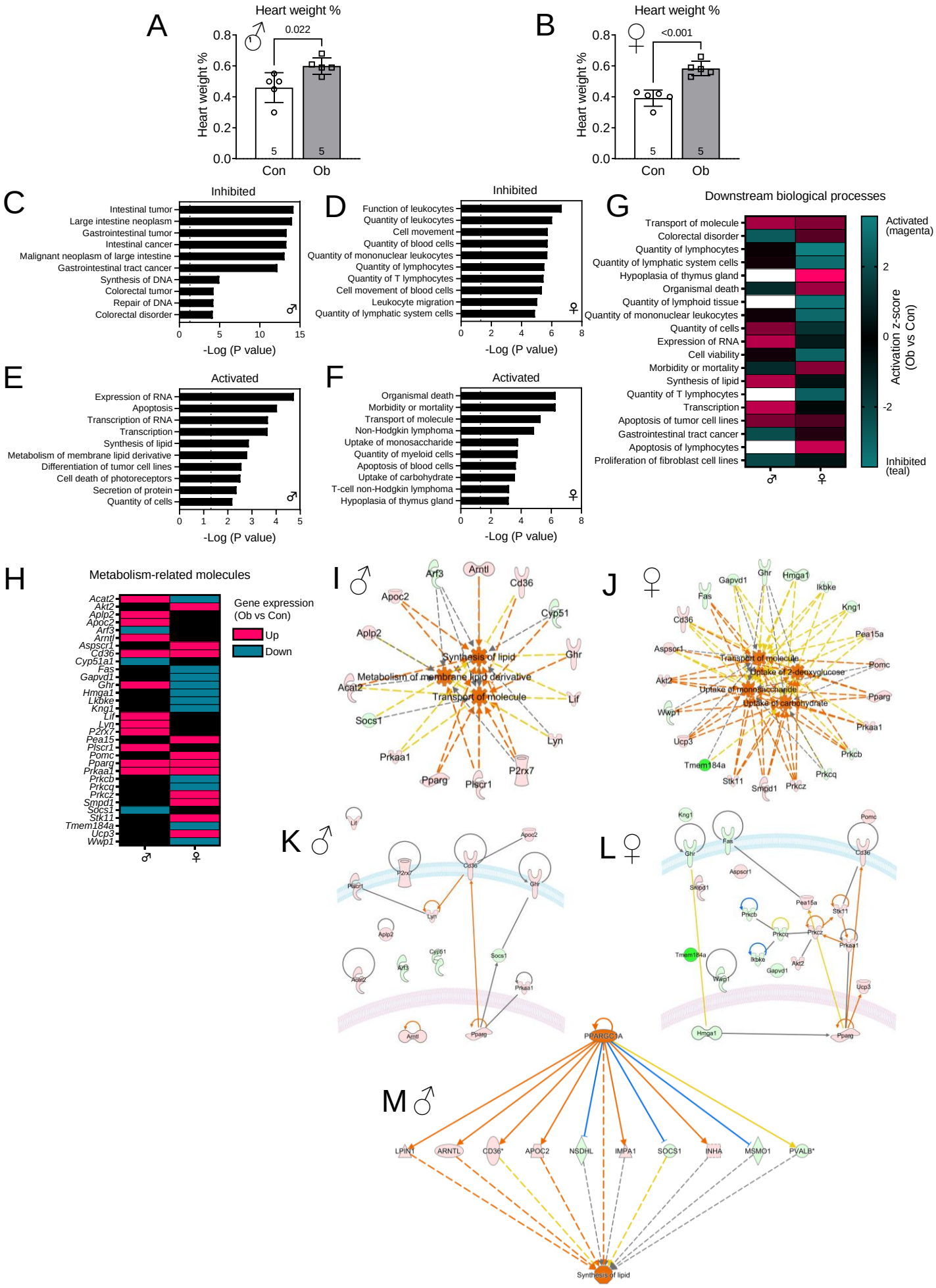

Fig. 2 Maternal obesity causes age- and sex-dependent left ventricular diastolic dysfunction in adult offspring. ○ Control □ Obese

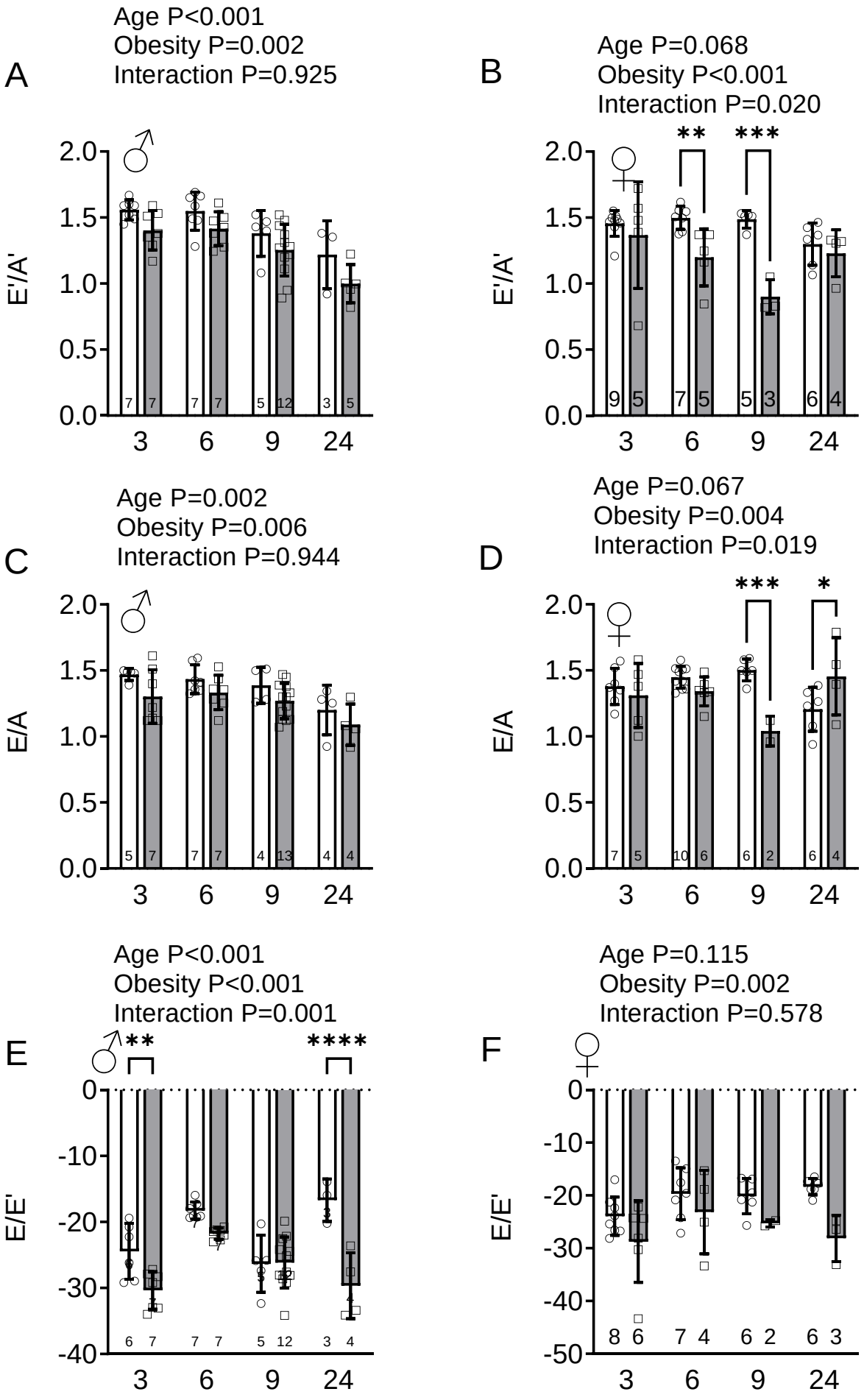

Fig. 3 Maternal obesity causes age- and sex-dependent left ventricular dilatation in adult offspring.

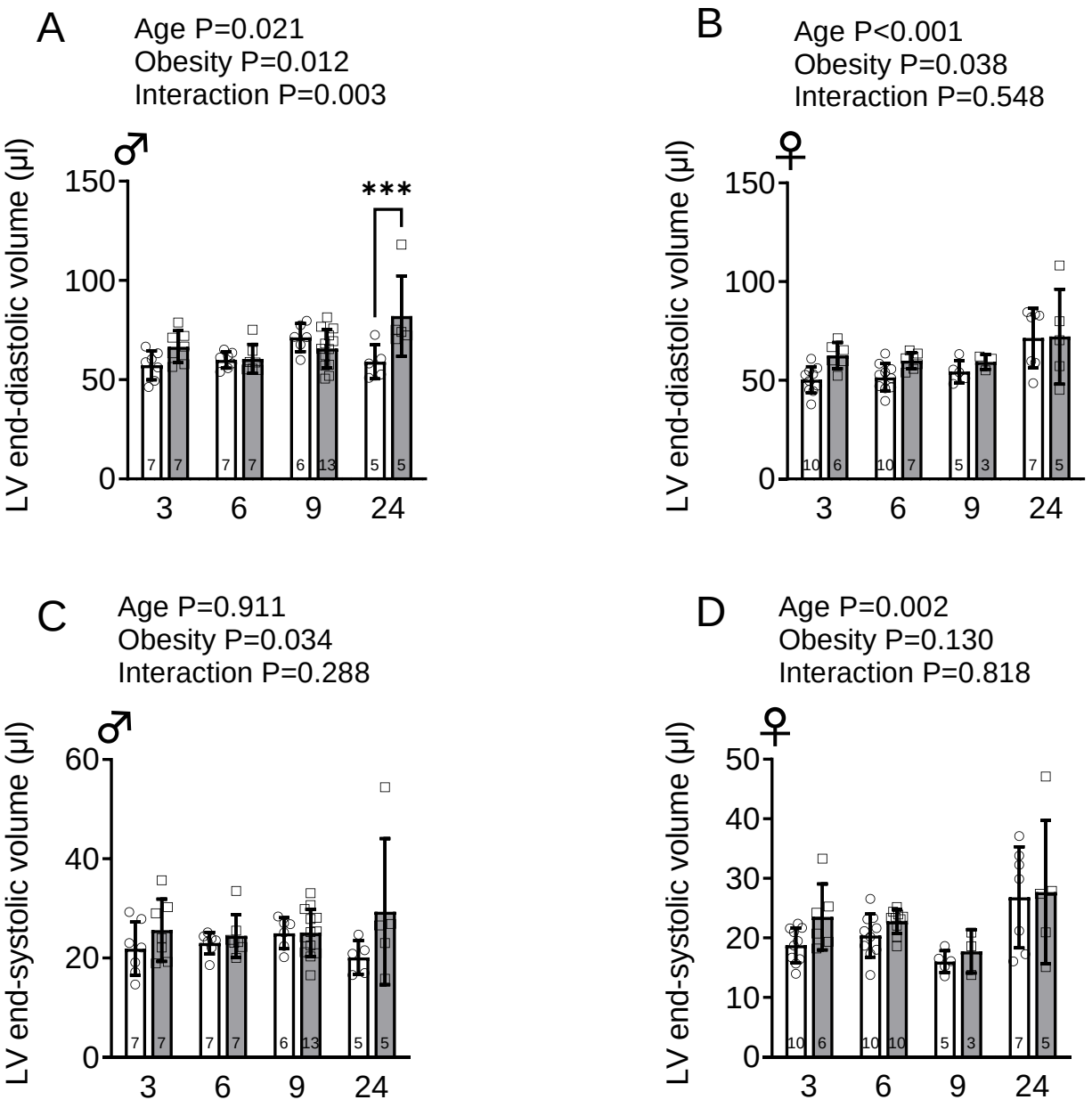

Fig. 4 Maternal obesity increases cardiac expression of Pparg and its downstream targets in adult offspring.

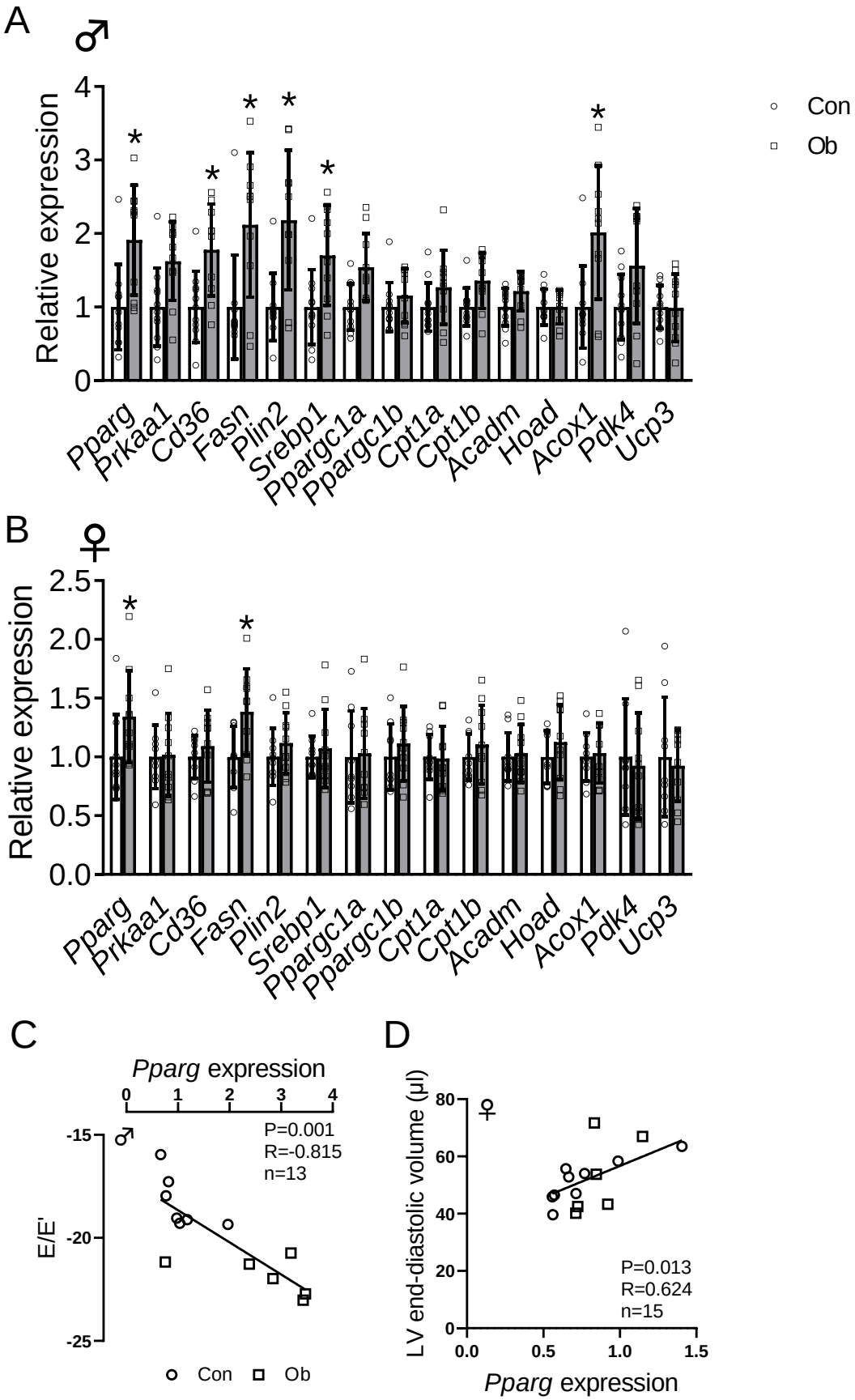

Fig. 5 Correlations between cardiac expression of metabolism-related genes and echocardiographic indices in female offspring of control and obese dams.

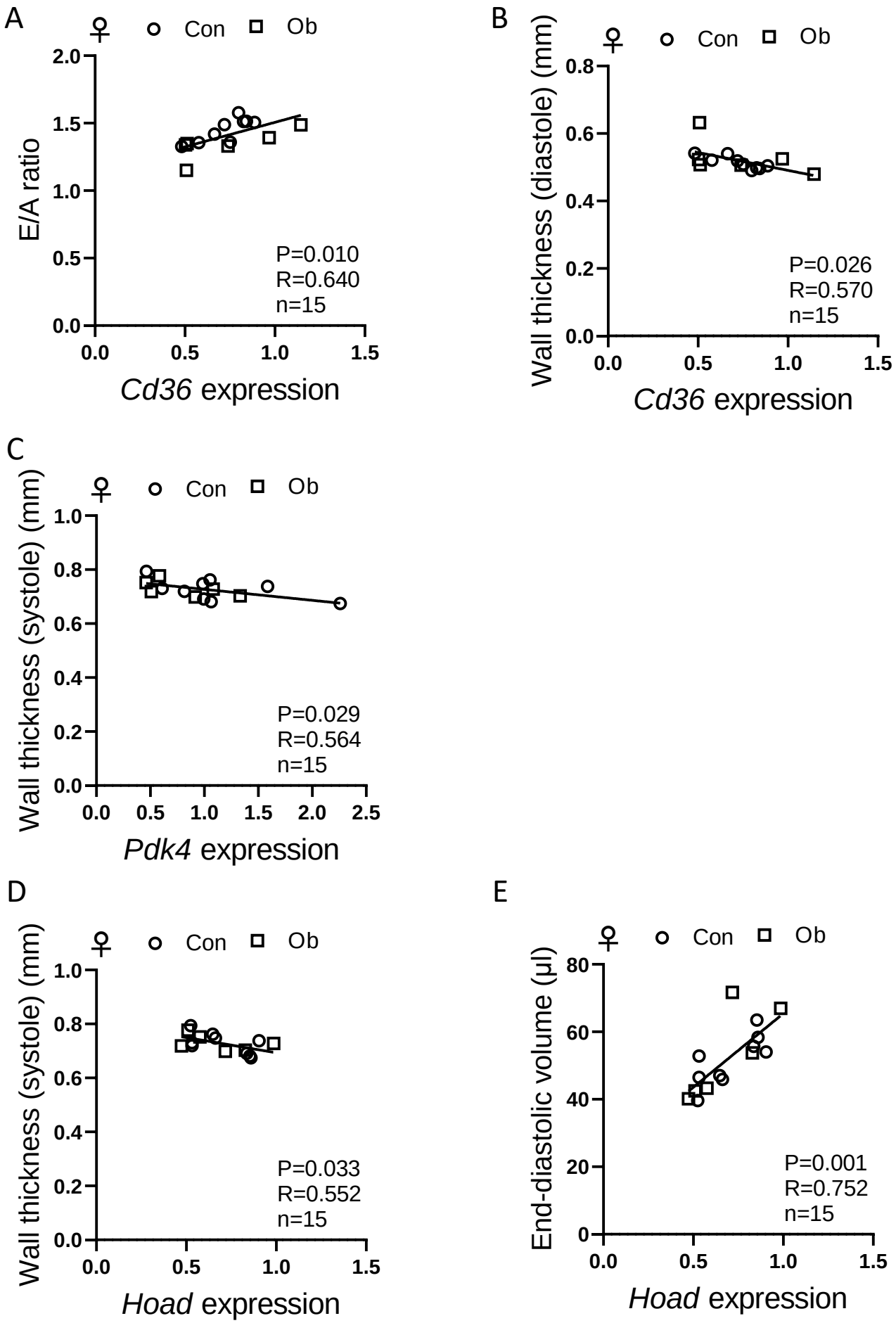

Fig. 6 Maternal obesity increases myocardial fatty acid oxidation in adult male, but not female, offspring

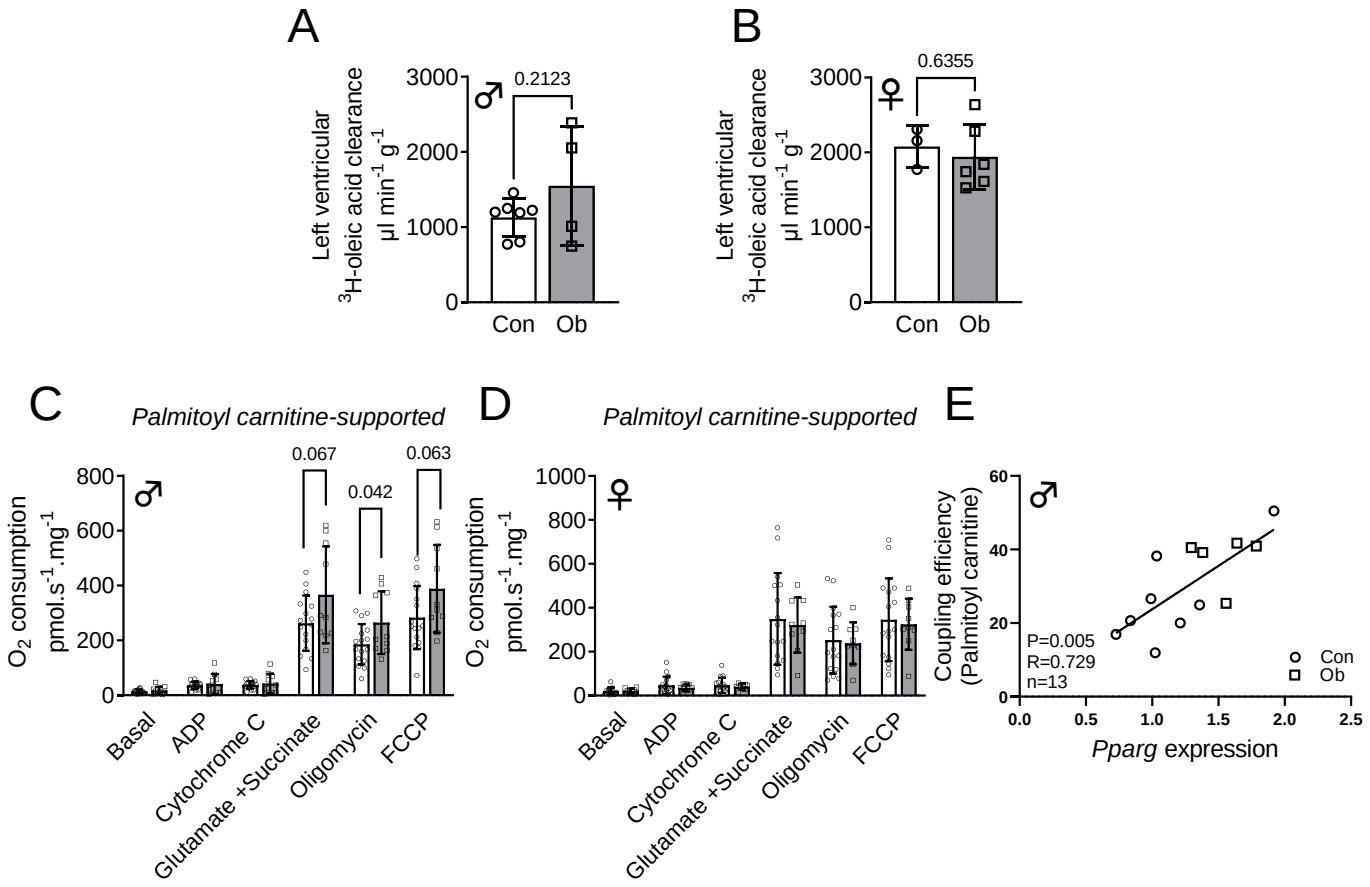

Fig. 7 Representative western blots for fatty acid transporter, glucose transporter and insulin receptor proteins in hearts of 6-month-old offspring of control and obese dams

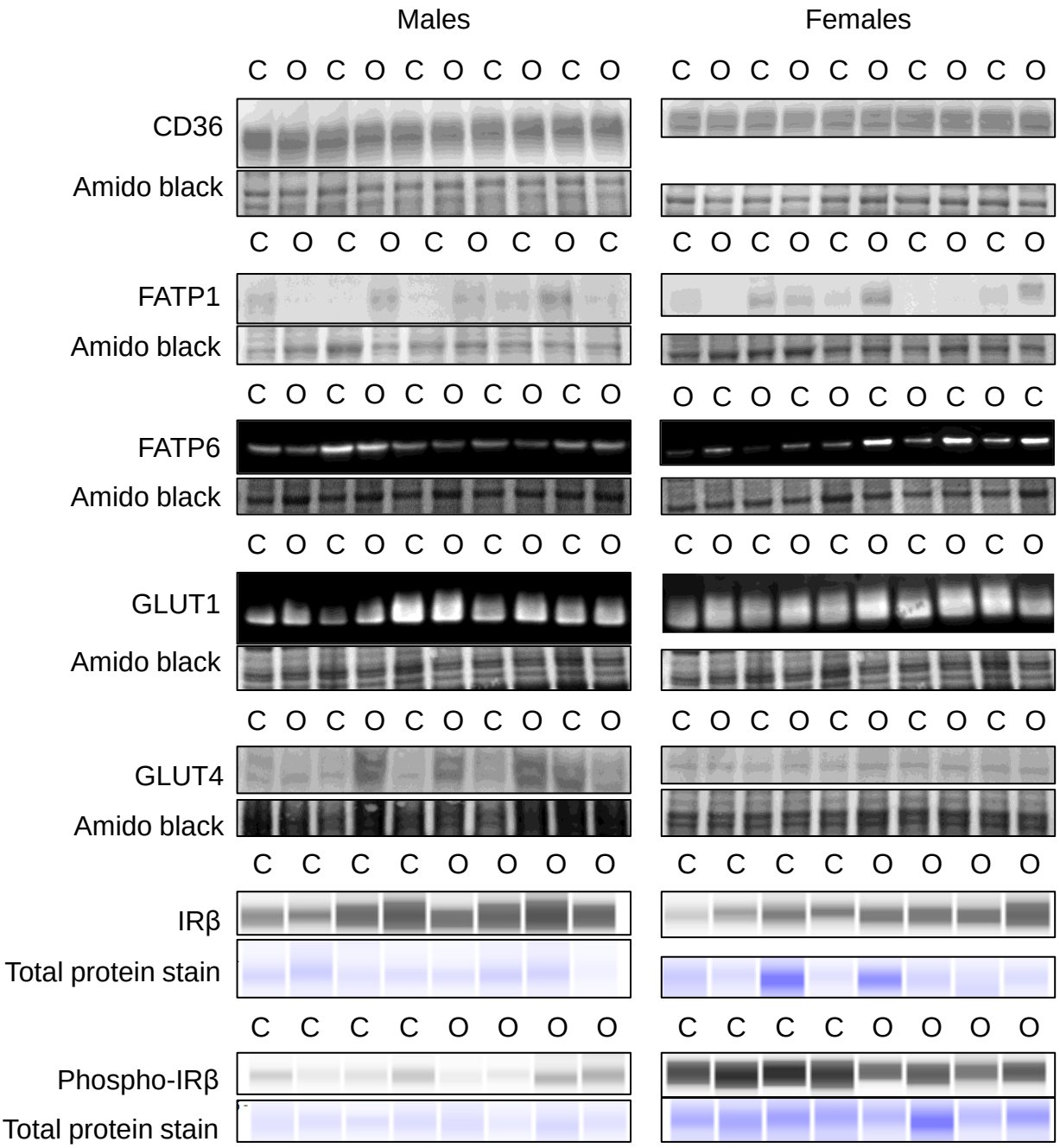

Fig. 8 Maternal obesity impairs myocardial glucose uptake in adult female, but not male, offspring

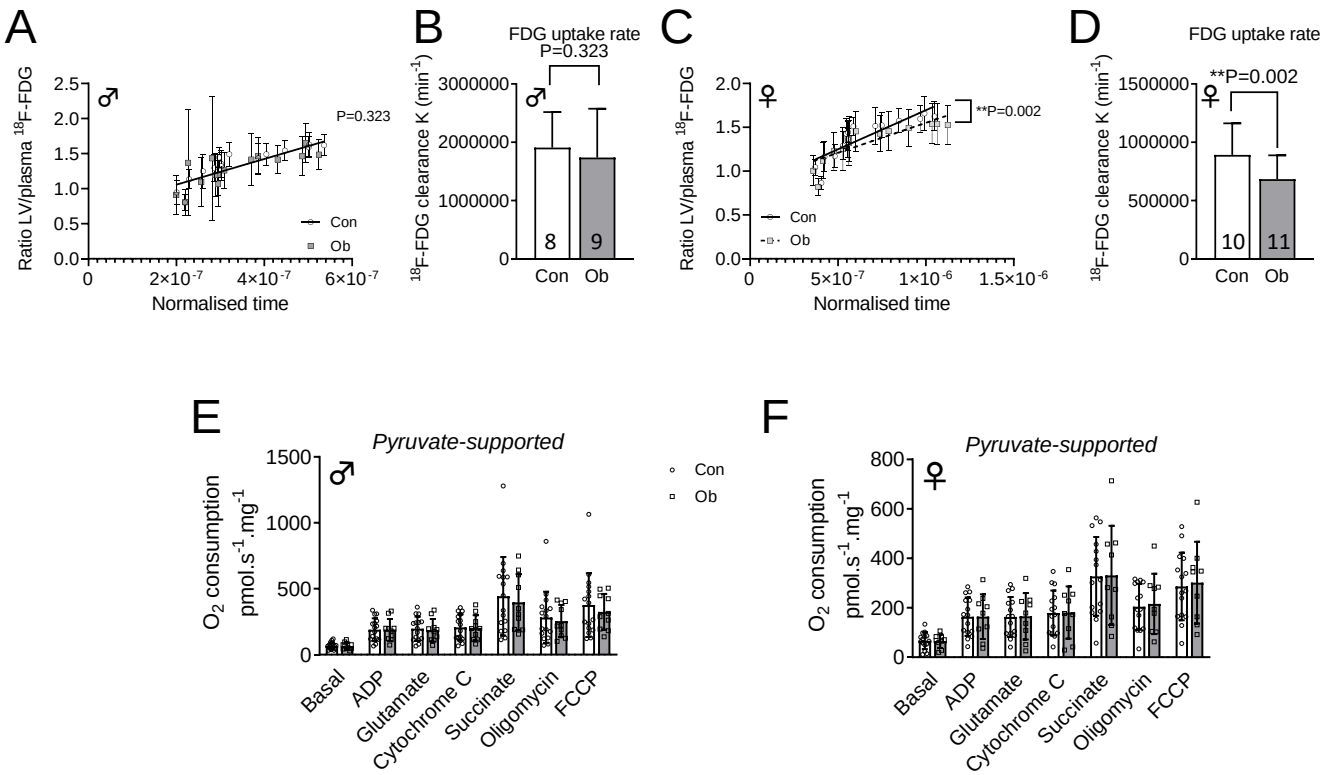

Fig. 9 Maternal obesity does not affect myocardial histone H3 acetylation in adult offspring.